Supporting Information

Non-fullerene acceptors with hetero-dihalogenated terminals induce significant difference in single crystallography and enable binary organic solar cells with 17.5% efficiency

Lai Wang, Qiaoshi An,* Lu Yan, Hai-Rui Bai, Mengyun Jiang, Asif Mahmood, Can Yang, Hongfu Zhi and Jin-Liang Wang*

Key Laboratory of Cluster Science of Ministry of Education, Beijing Key Laboratory of Photoelectronic/Electrophotonic Conversion Materials, School of Chemistry and Chemical Engineering, Beijing Institute of Technology, Beijing, 100081, China.
E-mail: qsan@bit.edu.cn; jinlwang@bit.edu.cn

1. Supplemental Experimental Procedures

Materials and Characterization:

All air and water-sensitive reactions were carried out under N_2. The other precursors were used as the common commercial level. ^{1}H and ^{13}C NMR spectra were carried out on a Bruker Ascend-400 and 700 NMR spectrometer. All chemical shifts were reported in ppm. Chemical shifts in ^{1}H NMR were referenced to TMS and in ^{13}C NMR were referenced to $CDCl_3$ and d_6-DMSO. The peaks positions of ^{13}C NMR were marked by groups. MALDI-TOF-MS was recorded on a Bruker BIFLEX III mass spectrometer. HR-FI-MS measurements were carried out at Bruker Solarix XR FTMS. Thermogravimetric analysis (TGA) was performed using a TA Instrument Q600 analyzer under nitrogen gas flow with a heating rate of 10 ºC min^{-1}. UV-vis absorption spectra were taken on Hitachi UH5300 UV-vis spectrometer. The electrochemical cyclic voltammetry was carried out on CHI electrochemical workstation with glass carbon disk, Ag/Ag$^+$ electrode, and Pt wire, as working electrode, reference electrode, and counter electrode, respectively, in acetonitrile solution with 0.1 M n-Bu_4NPF_6 as supporting electrolyte. Single crystals data collection of **Y-BO-FCl**, **Y-BO-FBr**, and **Y-BO-ClBr** was performed at 100 K or 170 K on a Super Nova diffractometer, using graphite-monochromated Cu Kα radiation (λ=1.54184 Å). All calculations were performed using the SHELXL and the crystallographic software package. There is not any no A-alert in CIF file of single crystal data for **Y-BO-FCl**, **Y-BO-FBr**, and **Y-BO-ClBr**. Crystallographic data have been deposited with the Cambridge Crystallographic Data Centre as supplementary publication No. CCDC 2062921, 2062922 and 2070537 for **Y-BO-FCl**, **Y-BO-FBr**, and **Y-BO-ClBr**, respectively. The single crystal X-ray crystallographic data were summarized in **Table S2**.

Atomic force microscopy (AFM) measurements were taken on a Dimension Icon AFM (Bruker) in tapping mode. Transmission electron microscope (TEM) measurements were performed using a JEOL JEM-1400 transmission electron microscope operated at 80 kV accelerating voltage. The samples for AFM and TEM characterization were prepared under the same conditions compared with the active layers of the PSCs. The samples for TEM measurement were displaced in deionized water and the active layers were picked up by using 400-mesh copper TEM grids. Grazing incidence X-ray diffraction (GIXD) measurements were performed at beamline BL14B1 of the Shanghai Synchrotron Radiation Facility (SSRF).

OSCs fabrication and measurement:

The patterned indium tin oxide (ITO) coated glass substrates (purchased from South China Science & Technology Company Limited , Size of 15*15*1mm, film thickness of 135nm, sheet

resistance 15 Ω sq^{-1}) were consecutively cleaned in ultrasonic baths containing detergent (Alconox), de-ionized water and ethanol, respectively. Then, PEDOT:PSS (Heraeus Clevios P VP AI 4083) thin films were fabricated on the cleaned ITO substrates by spin-coating method at 5000 round per minute (RPM) for 40 s, and then annealed at 150 °C for 10 minutes in the air conditions. After annealing treatment, ITO substrates coated with PEDOT:PSS films were transferred to a high purity nitrogen filled glove box. A blend solutions of **PM6: NFAs** (**Y-BO-FCl, Y-BO-FBr** or **Y-BO-ClBr**) (1:1.2, w/w) in chlorobenzene were spin-coated on PEDOT:PSS films in a high purity nitrogen filled glove box to fabricate the active layers. The active layers were annealed at 80 °C for 5 min. The optimized thickness of the active layer is ~110 nm, which was measured by Ambios Technology XP-2 stylus Profiler. After that, PDIN solution (2 mg ml^{-1} in methanol with 0.25 vol% acetic acid) was spin-coated on the top of active layers at 5000 RPM for 30 s. The 100 nm Ag cathode was deposited by thermal evaporation with a shadow mask under 10^{-4} Pa vacuum conditions and the thickness was monitored by a quartz crystal microbalance. The device area was exactly fixed at 4.0 mm^2. The current-voltage (I-V) curves of PSCs were measured in a high-purity nitrogen-filled glove box using a Keithley B2901A source meter. AM 1.5G irradiation at 100 mW cm^{-2} is provided by simulator (SS-F5-3A, Enlitech, AAA grade, 70×70 mm^2 photobeam size) in glove box, which was calibrated by standard silicon solar cells (purchased from Enlitech). The external quantum efficiency (EQE) spectra of PSCs were measured in air conditions by a solar cell spectral response measurement system (QE-R3011, Enlitech).

SCLC mobility measurement (SCLC)

The structure of electron-only devices is ITO/ZnO/active layer/PDIN/Al and the structure of hole-only devices is ITO/PEDOT:PSS/active layer/MoO_3/Ag. The fabrication conditions of the active layer films are same with those for the OSCs. The charge mobilities are generally described by the Mott-Gurney equation:

$$J = \frac{9\varepsilon_0\varepsilon_r\mu_0 V^2}{8L^3} exp\left(0.89\beta\sqrt{\frac{V}{L}}\right)$$

where J is the current density, L is the film thickness of the active layer, μ is the hole or electron mobility, ε_0 is the permittivity of free space (8.85×10^{-11} mF/cm), ε_r is the relative dielectric constant, $V=V_{app}-V_{bi}$ is the internal voltage in the device, where V_{app} is the applied voltage and V_{bi} is the built-in voltage reflecting the difference of work functions of the two electrodes. The charge mobilities were estimated using the following equation:

$$\ln\left(\frac{J}{V^2}\right) = \frac{0.89\gamma}{\sqrt{L}}\sqrt{V} + ln(\frac{9\varepsilon_0\varepsilon_r\mu}{8L^3})$$

2. Materials and Detailed Synthesized Procedures

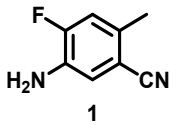

1

Compound 1: Conc. nitric acid (6 mL) was gradually added into the mixture of 4-fluoro-2-methylbenzonitrile (9 g, 66.6 mmol) and conc. sulfuric acid (20 mL) at 0 °C for 2h. The reaction mixture was poured into 100 ml water. The solid was filtered and the residue was recrystallization in ethanol. Then, a mixture of obtained solid and Sn (11.7 g, 98.8 mmol) in water (82 mL) was added conc. hydrochloric acid (33 mL). The reaction mixture was heated at 55 °C for 6 h. Then the mixture was cooled to 0 °C and solid $NaHCO_3$ was added slowly. The mixture was filtered and the residue was washed by dichloromethane. The combined filtrates

were extracted with dichloromethane and dried over anhydrous Na_2SO_4. After removal of the solvent and the product was obtained as white solid (6.74 g, 67.3%). This synthesis refers to similar compound in literature.[S1] ^{1}H NMR ($CDCl_3$, 400 MHz, ppm): δ 6.97-6.99 (d, J = 8.4 Hz, 1H, Ph-H), 6.90-6.93 (d, J = 11.2 Hz, 1H, Ph-H), 3.79 (s, 2H, NH_2), 2.41 (s, 3H, CH_3). ^{13}C NMR ($CDCl_3$, 100 MHz, ppm): δ (154.79, 152.32, J_{CF} = 247.2 Hz), (133.29, 133.15, J_{CF} = 13.9 Hz), (132.98, 132.90, J_{CF} = 7.6 Hz), 119.8, 117.8, (117.17, 116.97, J_{CF} = 19.8 Hz), (108.31, 108.27, J_{CF} = 3.4 Hz), 19.4.

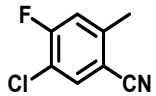

2a

Compound 2a: To a suspension of compound **1** (3.55 g, 23.6 mmol) in H_2O (13 mL) and conc. hydrochloric acid (30 mL) at 0 °C, $NaNO_2$ (2.12 g, 30.7 mmol) in H_2O (10 mL) was gradually added, followed by CuCl (3.51 g, 35.5 mmol) in conc. hydrochloric acid (10 mL) was added quickly. After warmed up to room temperature, the reaction was stirred for 30 min. The product was extracted with dichloromethane and dried over anhydrous Na_2SO_4. After removal of the solvent, the crude product was purified by silica gel column chromatography, eluting with petroleum ether/dichloromethane (8:1) by silica gel column chromatography, to give the product as white solid (3.07 g, 76.7%). ^{1}H NMR ($CDCl_3$, 400 MHz, ppm): δ 7.65-7.66 (d, J = 7.2 Hz, 1H, Ph-H), 7.11-7.13 (d, J = 9.2 Hz, 1H, Ph-H), 2.54 (s, 3H, CH_3). ^{13}C NMR ($CDCl_3$, 100 MHz, ppm): δ (161.59, 159.03, J_{CF} = 256.7 Hz), (143.53, 143.44, J_{CF} = 8.3 Hz), 134.5, (119.62, 119.43, J_{CF} = 18.8 Hz), (118.74, 118.52, J_{CF} = 21.8 Hz), 116.2, (109.88, 109.85, J_{CF} = 3.8 Hz), 20.2. HR-FT-MS (*m/z*): calcd for C_8H_5ClFN: 169.0167. Found: 170.0168 ($[M+H^+]^+$).

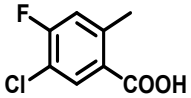

3a

Compound 3a: The mixture of compound **2a** (3.07 g, 18.1 mmol), H_2O (13 mL), conc. sulfuric acid (13 mL) and acetic acid (13 mL) were heated at 120 °C for 20 h. Then the reacted solution was poured into 20 mL H_2O, then the precipitate was filtered off and washed with petroleum ether to get white solid (3.05 g, 89.5%). The crude product can be used to the next step without further purification. ^{1}H NMR ($CDCl_3$, 400 MHz, ppm): δ 12.12 (br, 1H, COOH), 8.15-8.17 (d, J = 7.6 Hz, 1H, Ph-H), 7.05-7.08 (d, J = 9.2 Hz, 1H, Ph-H), 2.68 (s, 3H, CH_3). ^{13}C NMR ($CDCl_3$, 100 MHz, ppm): δ 171.2, (161.73, 159.18, J_{CF} = 255.4 Hz), (143.28, 143.20, J_{CF} = 8.2 Hz), 134.4, (125.07, 125.04, J_{CF} = 3.3 Hz), (119.94, 119.73, J_{CF} = 10.9 Hz), (118.59, 118.41, J_{CF} = 17.9 Hz), 21.9. HR-FT-MS (*m/z*): calcd for $C_8H_5ClFO_2$: 186.9968. Found: 186.9969 ($[M-H^+]^-$).

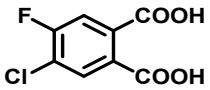

4a

Compound 4a: A mixture of compound **3a** (3.05 g, 16.2 mmol), $KMnO_4$ (5.11 g, 32.3 mmol) and KOH (1.36 g, 24.3 mmol) in H_2O (300 mL) was refluxed for 24 h. The reaction mixture was filtered to remove black solids, and the remaining filtrate was acidified to pH=1. After filtering, the filtrate was extracted with ethyl acetate and dried over anhydrous Na_2SO_4. After removal of the solvent, the crude product was obtained as white solid (2.26 g, 63.6%) and the crude product can be used to the next step without further purification. ^{1}H NMR (d_6-DMSO, 400 MHz, ppm): δ 13.02 (br, 1H, COOH), 7.95-7.96 (d, J = 7.2 Hz, 1H, Ph-H), 7.74-7.77 (d, J

= 8.4 Hz, 1H, Ph-H). ^{13}C NMR (d_6-DMSO, 100 MHz, ppm): δ 167.8, 167.4, (160.34, 157.83, J_{CF} = 250.8 Hz), (135.36, 135.29, J_{CF} = 7.0 Hz), 132.1, (131.01, 130.97, J_{CF} = 3.9 Hz), (123.02, 122.84, J_{CF} = 17.9 Hz), (118.06, 117.83, J_{CF} = 23.0 Hz). HR-FT-MS (*m/z*): calcd for $C_8H_3ClFO_4$: 216.9709. Found: 216.9709 ([M-H$^+$]$^-$)

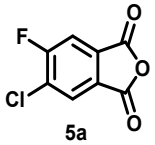

5a

Compound 5a: Compound **4a** (2.26 g, 10.3 mmol) in anhydrous acetic anhydride (10 mL) was refluxed for 10 h. After the temperature of reaction mixture is cooled to room temperature. The crude product was poured into petroleum ether (100 mL) and the precipitate was filtered off and washed with petroleum ether. The crude product was obtained as white solid (1.63 g, 78.9%), which can be used to the next step without further purification. ^{1}H NMR ($CDCl_3$, 400 MHz, ppm): δ 8.09-8.11 (d, J = 6.0 Hz, 1H, Ph-H), 7.76-7.78 (d, J = 6.8 Hz, 1H, Ph-H). ^{13}C NMR ($CDCl_3$, 100 MHz, ppm): δ (164.15, 161.54, J_{CF} = 262.0 Hz), 160.6, 160.5, (131.58, 131.49, J_{CF} = 9.1 Hz), (131.24, 131.04, J_{CF} = 19.8 Hz), 128.4, (127.73, 127.70, J_{CF} = 3.5 Hz), (113.83, 113.58, J_{CF} = 24.6 Hz). HR-FT-MS (*m/z*): calcd for $C_8H_3ClFO_3$: 200.9749. Found: 200.9747 ([M+H$^+$]$^+$).

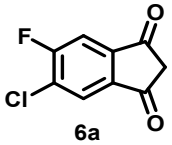

6a

Compound 6a: The mixture of compound **5a** (3.15 g, 15.7 mmol), ethyl acetoacetate (2.18 mL, 17.3 mmol), acetic anhydride (15 mL) and trimethylamine (15 mL), were heated at 65 °C under N_2 atmosphere for 10 h. Then, ice-water (10 mL) and conc. hydrochloric acid (10 mL) were poured into reaction mixture, and the mixture was heated at 80 °C for 1 h. After cooling to room temperature, the precipitate was filtered, washed with water and petroleum ether, dried to get the crude product yellow solid (3.13 g, 71.7%), which can be used to the next step without further purification.

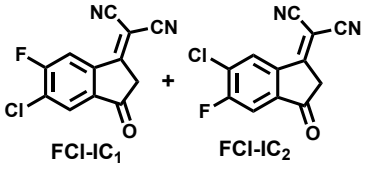

FCl-IC$_1$ FCl-IC$_2$

FCl-IC$_1$ and **FCl-IC$_2$:** In a 100 mL round-bottom flask, anhydrous sodium acetate (1.23 g, 15 mmol) was added to a solution of compound **6a** (1.82 g, 10 mmol) and malononitrile (1.32 g, 20 mmol) in 30 mL of anhydrous EtOH. The reaction mixture was stirred at room temperature for 12 h. Then the mixture was acidified by conc. hydrochloric acid and extracted with dichloromethane, and dried over anhydrous Na_2SO_4. After removal of the solvent, the crude product was purified by silica gel column chromatography, eluting with petroleum ether /dichloromethane (1:2), to obtain the product with two isomers (**FCl-IC$_1$: FCl-IC$_2$** ≈ 1: 0.19) as gray solid (1.81 g, 78%).^{1}H NMR ($CDCl_3$, 400 MHz, ppm): δ 8.71-8.73 (d, J = 6.0 Hz, 0.16H, Ph-H), 8.38-8.40 (d, J = 8.4 Hz, 0.84H, Ph-H), 8.03-8.05 (d, J = 6.8Hz, 0.84H, Ph-H), 7.69-7.70 (d, J = 6.8 Hz, 0.16H, Ph-H), 3.76 (s, 2H, CH_2). ^{13}C NMR ($CDCl_3$, 100 MHz, ppm): δ 192.5, 192.0, 163.85, 163.83, (163.64, 161.03, J_{CF} = 261.1 Hz), 163.56, (142.13, 142.03, J_{CF} = 9.2 Hz), (141.18, 141.11, J_{CF} = 7.5 Hz), (138.70, 138.67, J_{CF} = 3.4 Hz), (137.18, 137.16, J_{CF} = 2.8 Hz), (131.22, 131.02, J_{CF} = 20.0 Hz), (131.15, 130.95, J_{CF} = 20.0 Hz), 128.5, 127.1,

(113.57, 113.32, J_{CF} = 24.9 Hz), (112.07, 111.84, J_{CF} = 22.6 Hz), 111.7, (111.56, 111.48, J_{CF} = 8.5 Hz), 80.7, 80.0, 43.3, 43.1. HR-FT-MS (*m/z*): calcd for $C_{12}H_3ClFN_2O$: 244.9923. Found: 244.9927 ($[M+H^+]^+$).

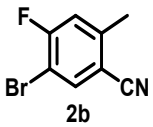

2b

Compound 2b: To a suspension of compound **1** (4.05 g, 27.0 mmol) in H_2O (15 mL) and 8.6 M hydrobromic acid (20 mL) at 0 °C, $NaNO_2$ (2.42 g, 35.0 mmol) in H_2O (10 mL) was gradually added, followed by CuBr (5.80 g, 40.4 mmol) in 8.6 M hydrobromic acid (15 mL) was added quickly. After warmed up to room temperature, the reaction was stirred for 0.5 h. The product was extracted with dichloromethane and dried over anhydrous Na_2SO_4. After removal of the solvent, the crude product was purified by silica gel column chromatography, eluting with petroleum ether /dichloromethane (8:1), to give the product **2b** as white solid (3.93 g, 68.2%). ^{1}H NMR ($CDCl_3$, 400 MHz, ppm): δ 7.76-7.78 (d, J = 6.4 Hz, 1H, Ph-H), 7.07-7.09 (d, J = 9.2 Hz, 1H, Ph-H), 2.51 (s, 3H, CH_3). ^{13}C NMR ($CDCl_3$, 100 MHz, ppm): δ (162.54, 159.99, J_{CF} = 254.9 Hz), (144.27, 144.18, J_{CF} = 8.5 Hz), 137.3, (118.48, 118.25, J_{CF} = 23.1 Hz), 116.0, (110.32, 110.29, J_{CF} = 3.7 Hz), (106.85, 106.63, J_{CF} = 22.2 Hz), 20.2.

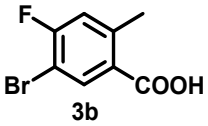

3b

Compound 3b: The synthetic route of **3b** is similar with that of **3a,** excepting for using **2b** to replace **2a,** to give the product as white solid (yield: 87.4%). ^{1}H NMR ($CDCl_3$, 400 MHz, ppm): δ 12.12 (br, 1H, COOH), 8.30-8.31 (d, J = 7.2 Hz, 1H, Ph-H), 7.03-7.05 (d, J = 9.2 Hz, 1H, Ph-H), 2.63 (s, 3H, CH_3). ^{13}C NMR ($CDCl_3$, 100 MHz, ppm): δ 171.2, (162.78, 160.24, J_{CF} = 253.9 Hz), (144.08, 144.00, J_{CF} = 8.3 Hz), 137.3, (125.51,125.48, J_{CF} = 3.3 Hz), (119.79, 119.57, J_{CF} = 22.1 Hz), (106.10, 105.89, J_{CF} = 21.2 Hz), 22.0.

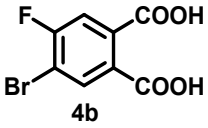

4b

Compound 4b: The synthetic route of **4b** is similar with that of **4a,** excepting for using **3b** to replace **3a,** to give the product as white solid, yield: 69.0%.[S2] ^{1}H NMR (d_6-DMSO, 400 MHz, ppm): δ 13.20 (br, 1H, COOH), 8.04-8.06 (d, 1H, J = 6.8 Hz, Ph-H), 7.67-7.69 (d, 1H, J = 8.8 Hz, Ph-H). ^{13}C NMR (d_6-DMSO, 100 MHz, ppm): δ 167.5, 167.0, (161.14, 158.65, J_{CF} = 249.1 Hz), (135.72, 135.65, J_{CF} = 7.0 Hz), 134.6, (130.76, 130.72, J_{CF} = 3.7 Hz), (117.36, 117.11, J_{CF} = 24.4 Hz), (111.24, 111.03, J_{CF} = 21.4 Hz).

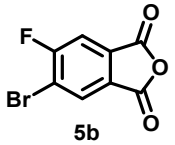

5b

Compound 5b: The synthetic route of **5b** is similar with that of **5a,** excepting for using **4b** to replace **4a**, to give the product as white solid, yield: 76.3%.[S2] ^{1}H NMR ($CDCl_3$, 400 MHz, ppm): δ 8.25-8.27 (d, J = 5.6 Hz, 1H, Ph-H), 7.71-7.73 (d, J = 6.0 Hz, 1H, Ph-H). ^{13}C NMR ($CDCl_3$, 100 MHz, ppm): δ (165.12, 162.52, J_{CF} = 260.1 Hz), 160.8, 160.4, (132.47,132.38, J_{CF}

= 9.2 Hz), 131.5, (127.93, 127.89, J_{CF} = 3.4 Hz), (119.62, 119.39, J_{CF} = 23.4 Hz), (113.52, 113.26, J_{CF} = 26.0 Hz).

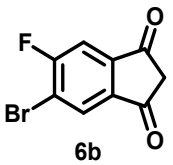

6b

Compound 6b: The synthetic route of **6b** is similar with that of **6a**, excepting for using **5b** to replace **5a**, to give the product as yellow solid (83.2%), which can be used to the next step without further purification.

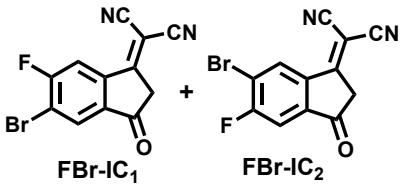

FBr-IC$_1$ **FBr-IC$_2$**

FBr-IC$_1$ and **FBr-IC$_2$:** The synthetic route of **FBr-IC** is similar with that of **FCl-IC,** excepting for using **6b** to replace **6a**. The crude product was purified by silica gel column chromatography, eluting with petroleum ether/dichloromethane (1:2) to give the product as gray solid with two isomers (**FBr-IC$_1$: FBr-IC$_2$** = 1: 0.67), yield: 72.5%.[S2] ^{1}H NMR ($CDCl_3$, 400 MHz, ppm): δ 8.87-8.89 (d, J = 5.6 Hz, 0.40H, Ph-H), 8.32-8.34 (d, J = 7.6 Hz, 0.60H, Ph-H), 8.20-8.21 (d, J = 6.4 Hz, 0.60H, Ph-H), 7.64-7.66 (d, J = 6.4 Hz, 0.40H, Ph-H), 3.76 (s, 2H, CH_2). ^{13}C NMR ($CDCl_3$, 100 MHz, ppm): δ 192.6, 191.9, (164.60, 162.01, J_{CF} = 259.4 Hz), (164.61, 161.99, J_{CF} = 262.3 Hz), 163.9, 163.4, (142.87, 142.78, J_{CF} = 9.4 Hz), (141.97, 141.89, J_{CF} = 10.8 Hz), (138.98, 138.94, J_{CF} = 3.3 Hz), (137.26, 137.23, J_{CF} = 2.7 Hz), 131.6, 130.3, (119.91, 119.67, J_{CF} = 23.3 Hz), (119.82, 119.58, J_{CF} = 23.4 Hz), 113.2, 113.0, (111.71, 111.58, J_{CF} = 12.7 Hz), 111.5, 80.8, 79.9, 43.4, 43.1.

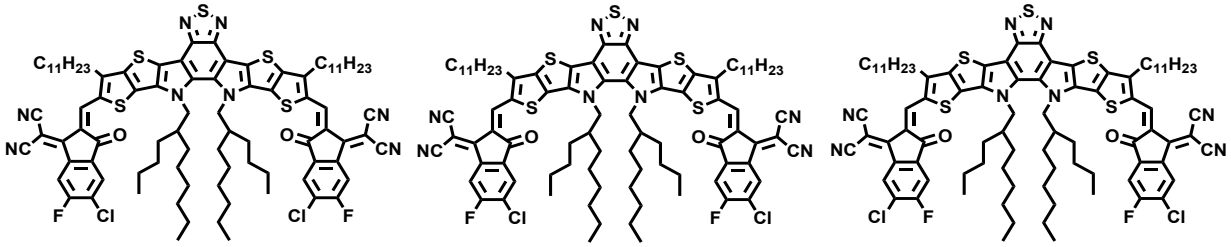

Y-BO-FCl-1 **Y-BO-FCl-2** **Y-BO-FCl-3**

Y-BO-FCl: In a 100 mL two-neck round-bottom flask, **Y-BO-CHO** (92 mg, 0.08 mmol), **FCl-IC** (119 mg, 0.48 mmol) was added. The reaction mixture was evacuated and backfilled with N_2 three times, and then freshly degassed chloroform (30 mL) and pyridine (0.5 mL) were added into the reaction mixture. The reaction mixture was stirred at room temperature for 12 h. Then the reaction mixture was poured into methanol and the precipitate was filtered. The crude product was purified by silica gel column chromatography, eluting with petroleum ether/dichloromethane (3:2) to give the product with three regioisomers (**Y-BO-FCl-1, Y-BO-FCl-2, Y-BO-FCl-3)** as black solid (126 mg, 85.9%). ^{1}H NMR ($CDCl_3$, 400 MHz, ppm): δ 9.16 (s, 2H, C=CH), 8.77-8.78 (d, J = 6.0 Hz, 0.72H, Ph-H), 8.47-8.49 (d, J = 8.4 Hz, 1.28H, Ph-H), 7.93-7.95 (d, J = 6.8 Hz, 1.28H, Ph-H), 7.63-7.65 (d, J = 6.4 Hz, 0.72H, Ph-H), 4.76-4.78 (d, J = 7.6 Hz, 4H, CH_2), 3.21-3.24 (t, J = 6.8 Hz, 4H, CH_2), 2.10-2.16 (m, 2H, CH_2), 1.84-1.91 (m, 4H, CH_2), 1.47-1.53 (m, 4H, CH_2), 0.85-1.39 (m, 66H, CH_2, CH_3), 0.64-0.72 (m, 12H,

CH_3);^{13}C NMR ($CDCl_3$, 100 MHz, ppm): δ 186.1, 185.9, (162.36, 160.89, J_{CF} = 248.5 Hz), (162.24, 160.75, J_{CF} = 248.5 Hz), 158.5, 158.4, 153.9, 153.8, 147.4, 145.2, (139.82, 139.77, J_{CF} = 8.8 Hz), 137.7, 136.3, 136.2, 136.1, 135.3, 135.2, 134.2, 133.5, 133.41, 133.36, 130.9, (128.63, 128.52, J_{CF} = 19.1 Hz), (128.34, 128.23, J_{CF} = 19.4 Hz), 127.8, 125.7, 119.9, 119.7, 115.0, 114.6, 114.5, 113.7, (113.52, 113.37, J_{CF} = 25.7 Hz), (111.17, 111.04, J_{CF} = 22.8 Hz), 68.8, 68.5, 55.9, 39.3, 31.9, 31.7, 31.6, 31.2, 30.6, 30.5, 29.8, 29.7, 29.6, 29.5, 29.4, 28.1, 28.0, 25.6, 25.4, 22. 9, 22.7, 22.5, 14.1, 13.8. MALDI-TOF MS (*m/z*): calcd. for $C_{90}H_{102}Cl_2F_2N_8O_2S_5$: 1594.6. Found: 1595.8.

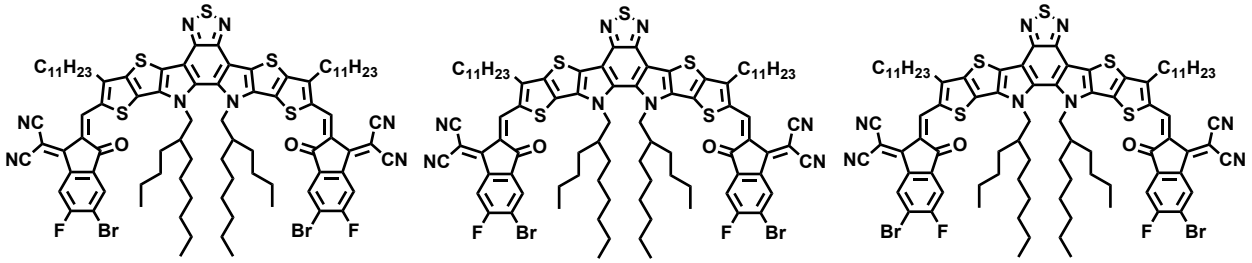

Y-BO-FBr-1 **Y-BO-FBr-2** **Y-BO-FBr-3**

Y-BO-FBr: The synthetic route of **Y-BO-FBr** is similar with that of **Y-BO-FCl,** excepting for using **FBr-IC** to replace **FCl-IC**. The crude product was purified by silica gel column chromatography, eluting with petroleum ether/dichloromethane (3:2) to give the product with three regioisomers (**Y-BO-FBr-1, Y-BO-FBr-2, Y-BO-FBr-3**) as black solid (yield: 87.5%). ^{1}H NMR ($CDCl_3$, 400 MHz, ppm): δ 9.14 (s, 2H, C=CH), 8.91 (d, J = 5.6 Hz, 0.60H, Ph-H), 8.42 (d, J = 8.4 Hz, 1.40H, Ph-H), 8.10 (d, J = 6.4Hz, 1.40H, Ph-H), 7.60 (d, J = 6.0 Hz, 0.60H, Ph-H), 4.79 (d, J = 7.2 Hz, 4H, CH_2), 3.21 (t, J = 7.0 Hz, 4H, CH_2), 2.13-2.16 (m, 2H, CH_2), 1.83-1.91 (m, 4H, CH_2), 1.47-1.54 (m, 4H, CH_2), 0.75-1.43 (m, 66H, CH_2, CH_3), 0.67-0.69 (m, 12H, CH_3). ^{13}C NMR ($CDCl_3$, 100 MHz, ppm): δ 186.2, 185.9, (163.44, 161.97, J_{CF} = 256.4 Hz), (163.30, 161.79, J_{CF} = 259.2 Hz), 158.7, 158.5, 154.0, 153.9, 147.5, 145.3, (140.77, 140.69, J_{CF} = 9.1 Hz), (138.59, 138.55, J_{CF} = 7.4 Hz), 137.7, 136.4, 136.3, 136.2, 135.5, 134.2, 133.7, 133.5, 131.0, 130.8, 128.8, 120.0, 119.8, (117.23, 117.10, J_{CF} = 22.8 Hz), (116.82, 116.69, J_{CF} = 22.9 Hz), 115.1, 114.6, 113.6, (113.35, 113.19, J_{CF} = 27.5 Hz), (110.92, 110.78, J_{CF} = 24.2 Hz), 68.8, 68.5, 55.8, 39.3, 31.9, 31.7, 31.6, 31.61, 31.2, 30.5, 29.8, 29.7, 29.6, 29.5, 29.4, 28.0, 27.9, 25.5, 25.4, 22.9, 22.8, 22.7, 22.5, 14.1, 14.0, 13.8. MALDI-TOF MS (*m/z*): calcd. for $C_{90}H_{102}Br_2F_2N_8O_2S_5$: 1683.4. Found: 1684.5.

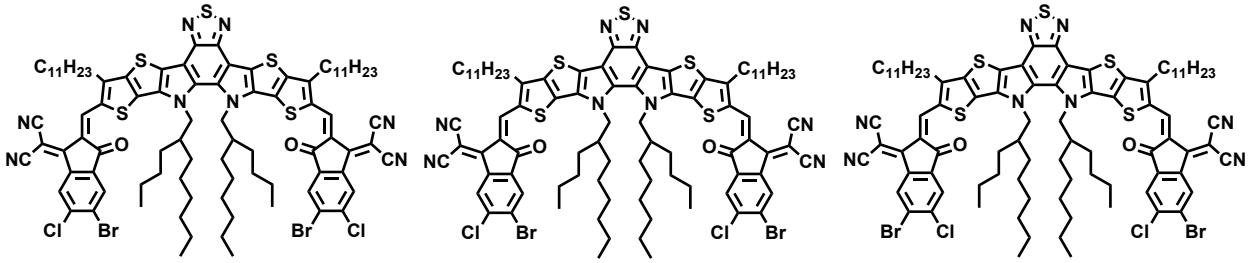

Y-BO-ClBr-1 **Y-BO-ClBr-2** **Y-BO-ClBr-3**

Y-BO-ClBr: The synthetic route of **Y-BO-ClBr** is similar with that of **Y-BO-FCl,** excepting for using **ClBr-IC** to replace **FCl-IC**. The crude product was purified by silica gel column chromatography, eluting with petroleum ether/dichloromethane (3:2) to give the product with three regioisomers (**Y-BO-ClBr-1, Y-BO-ClBr-2, Y-BO-ClBr-3**) as black solid (yield: 85.4%).[S3] ^{1}H NMR ($CDCl_3$, 400 MHz, ppm): δ 9.16 (s, 2H, C=CH), 8.96 (0.90H, Ph-H), 8.75

(1.10H, Ph-H), 8.13 (1.10H, Ph-H), 7.94 (0.90H, Ph-H), 4.78 (d, J = 7.2 Hz, 4H, CH_2), 3.22 (t, J = 7.6 Hz, 4H, CH_2), 2.11-2.17 (m, 2H, CH_2), 1.83-1.91 (m, 4H, CH_2), 1.47-1.53 (m, 4H, CH_2), 0.87-1.37 (m, 66H, CH_2, CH_3), 0.64-0.71 (m, 12H, CH_3).

3. Additional experimental results

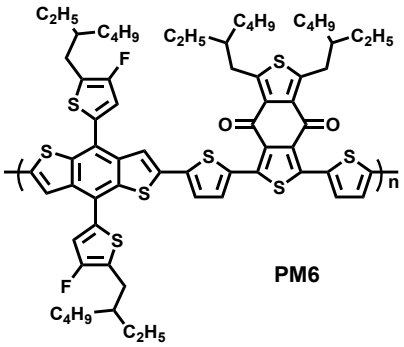

Figure S1. The molecular structure of donor **PM6**.

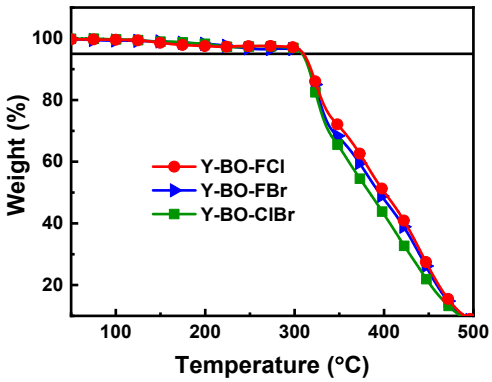

Figure S2. Thermal gravity analyzes (TGA) of **Y-BO-FCl**, **Y-BO-FBr**, and **Y-BO-ClBr** with a heating rate of 10 °C/min under N_2 atmosphere.

Table S1. DFT calculation results of **Y-BO-FCl**, **Y-BO-FBr**, and **Y-BO-ClBr** with all regioisomers, respectively.

Isomers	HOMO (eV)	LUMO (eV)	Potential energy (a.u.)	Diploe moment (Debye)
Y-BO-FCl-1	-3.61	-5.62	-6404.3012	0.2328
Y-BO-FCl-2	-3.61	-5.62	-6404.3006	0.4057
Y-BO-FCl-3	-3.61	-5.62	-6404.3000	0.5173
Y-BO-FBr-1	-3.60	-5.62	-10627.3207	0.8038
Y-BO-FBr-2	-3.59	-5.62	-10627.3202	0.8954
Y-BO-FBr-3	-3.58	-5.62	-10627.3196	0.9865
Y-BO-ClBr-1	-3.58	-5.61	-11348.0406	0.4865
Y-BO-ClBr-2	-3.58	-5.61	-11348.0405	0.4726

Y-BO-ClBr-3	-3.56	-5.61	-11348.0405	0.3312

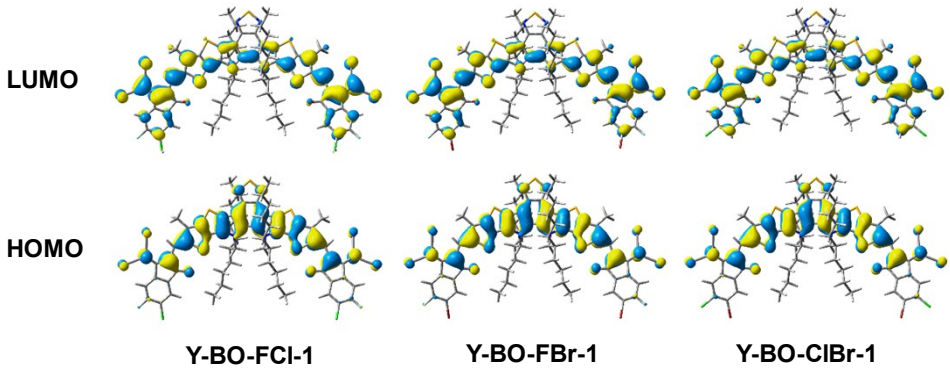

Figure S3. The conformation and distribution of frontier molecular orbital for the **Y-BO-FCl**, **Y-BO-FBr** and **Y-BO-ClBr** with lowest potential energy.

Table S2. Check CIF report of XRD data of single crystal of **Y-BO-FCl (**CCDC 2062921), **Y-BO-FBr** (CCDC 2062922), and **Y-BO-ClBr** (CCDC 2070537).

Compound		**Y-BO-FCl**	**Y-BO-FBr**	**Y-BO-ClBr**
Temperature		100 K	170 K	100 K
Bond precision		C-C = 0.0015 Å Wavelength=1.5418 Å	C-C = 0.0022 Å Wavelength=1.5418 Å	C-C = 0.0060 Å Wavelength=1.5418 Å
Cell	a (Å)	26.5046(10)	26.7059(7)	16.0896(6)
	b (Å)	23.0448(11)	23.0515(7)	17.7032(4)
	c (Å)	31.2654(18)	31.3331(11)	17.9514(5)
	α (°)	90	90	107.551
	β (°)	107.646(5)	107.898(3)	114.327
	γ (°)	90	90	90.288
Volume		18198.1(16)	18355.5(10)	4392.9(3)
Crystal system		Monoclinic	Monoclinic	Triclinic
Space group		*C 1 2/c 1*	*C 1 2/c 1*	*P -1*
Formula		$C_{90}H_{102}Cl_2F_2N_8O_2S_5$	$C_{90}H_{102}Br_2F_2N_8O_2S_5$	$C_{90}H_{102}Br_2Cl_2N_8O_2S_5$
Molecular Weight		1596.99	1685.91	1718.81
D_{calc}, g/cm^{-3}		1.166	1.210	1.299
Z		8	8	2
μ (mm^{-1})		2.131	2.593	3.236
F(000)		6768.0	7056.0	1796.0
h, k, l_{max}		33, 28, 39	33, 28, 39	18, 20, 21
Data completeness		0. 949	0.952	0.960
Theta(max)		75.565	75.380	64.999
R(reflections)		0.1347	0.1450	0.1572

wR_2(reflections)	0.4165	0.4303	0.4058
S	0.945	1.022	1.023
Npar	988	988	983

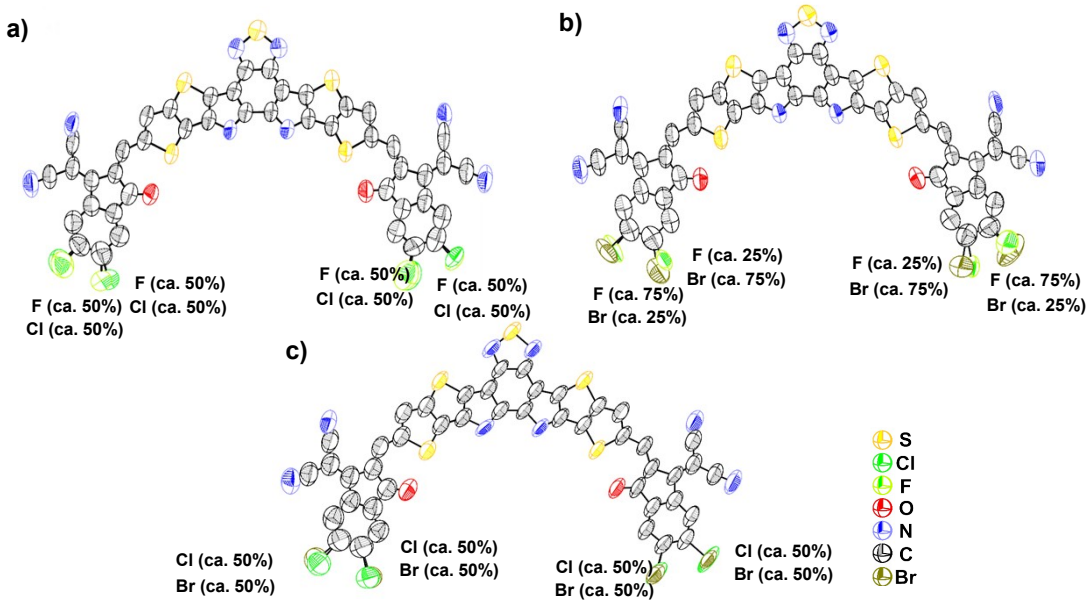

Figure S4. the ORTEP drawing of **Y-BO-FCl**, **Y-BO-FBr**, and **Y-BO-ClBr** crystal (displacement ellipsoid for terminal halogen atoms with ca. 50%/50% or ca. 75%/25%-occupancy depend on the different chemical regioselectivity of terminal halogen atoms and most reasonable atomic ellipsoid).

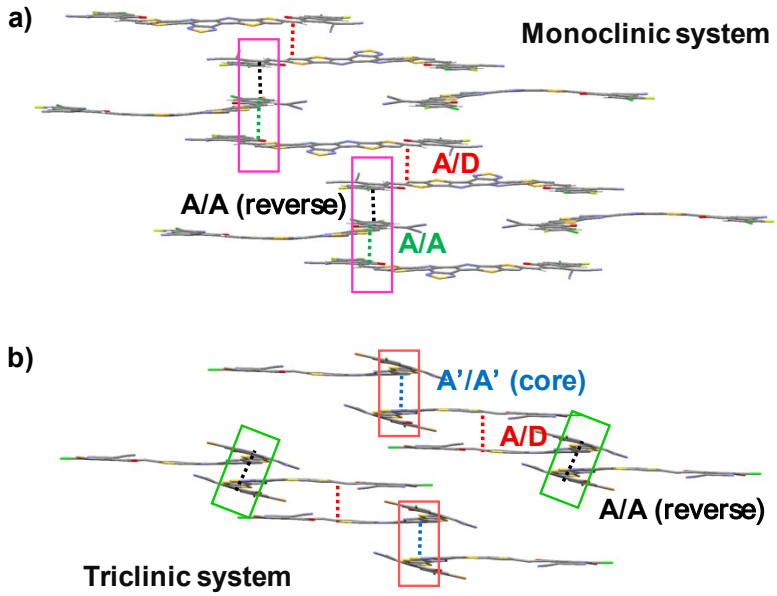

Figure S5. The vertical distribution of π-π interactions in different crystal system for (a) fluorine-based **Y-BO-FCl** and (b) nonfluorine-based **Y-BO-ClBr**.

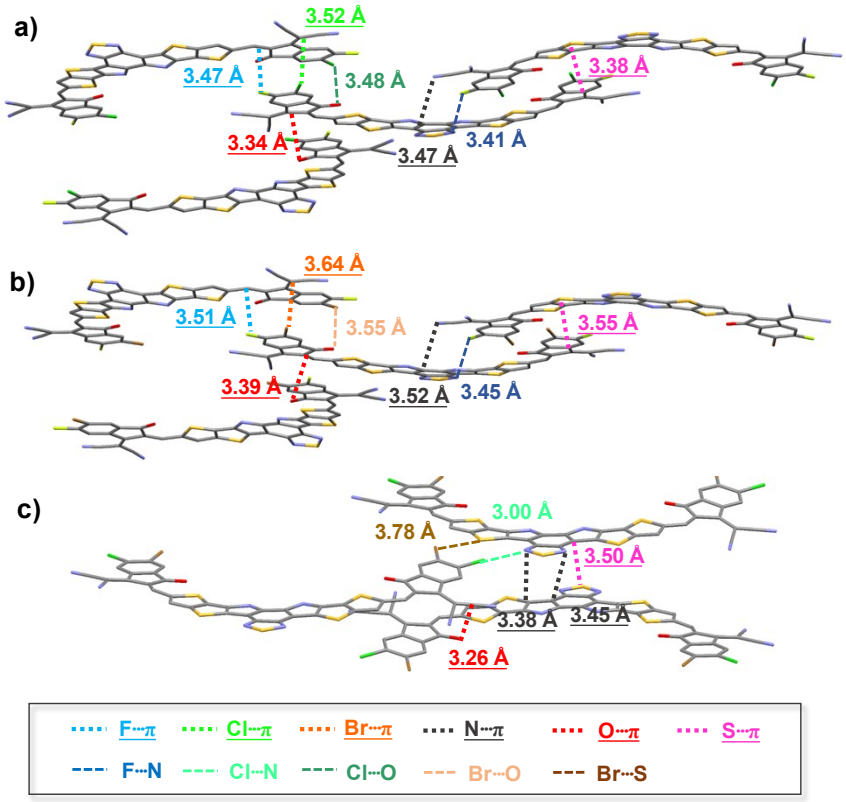

Figure S6. The intermolecular non-covalent interactions of (a) **Y-BO-FCl**, (b)**Y-BO-FBr** and (c)**Y-BO-ClBr** crystals.

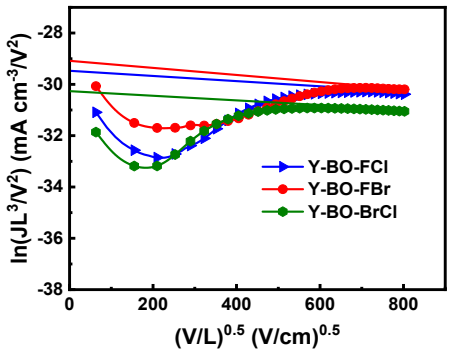

Figure S7. The $\ln(JL^3/V^2)$ vs $(V/L)^{0.5}$ curves of electron-only devices under dark condition for acceptor neat films by space-charge-limited current method.

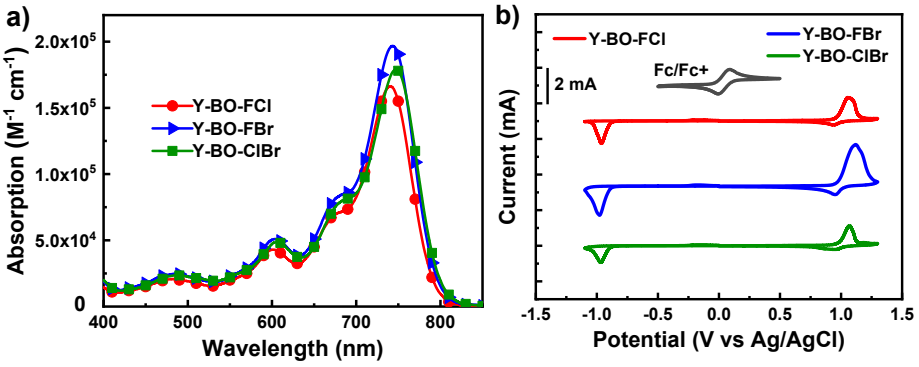

Figure S8. (a) Absorption spectra of acceptors in chloroform solution. (b) Cyclic voltammograms of **Y-BO-FCl, Y-BO-FBr** and **Y-BO-ClBr** films.

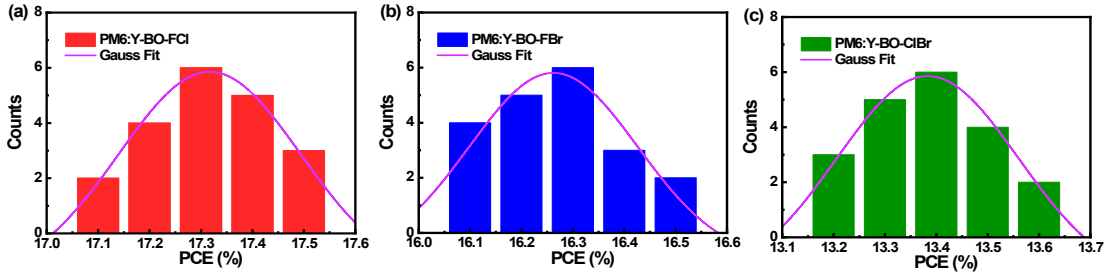

Figure S9. PCE distribution histogram of three typical OSCs according to 20 samples.

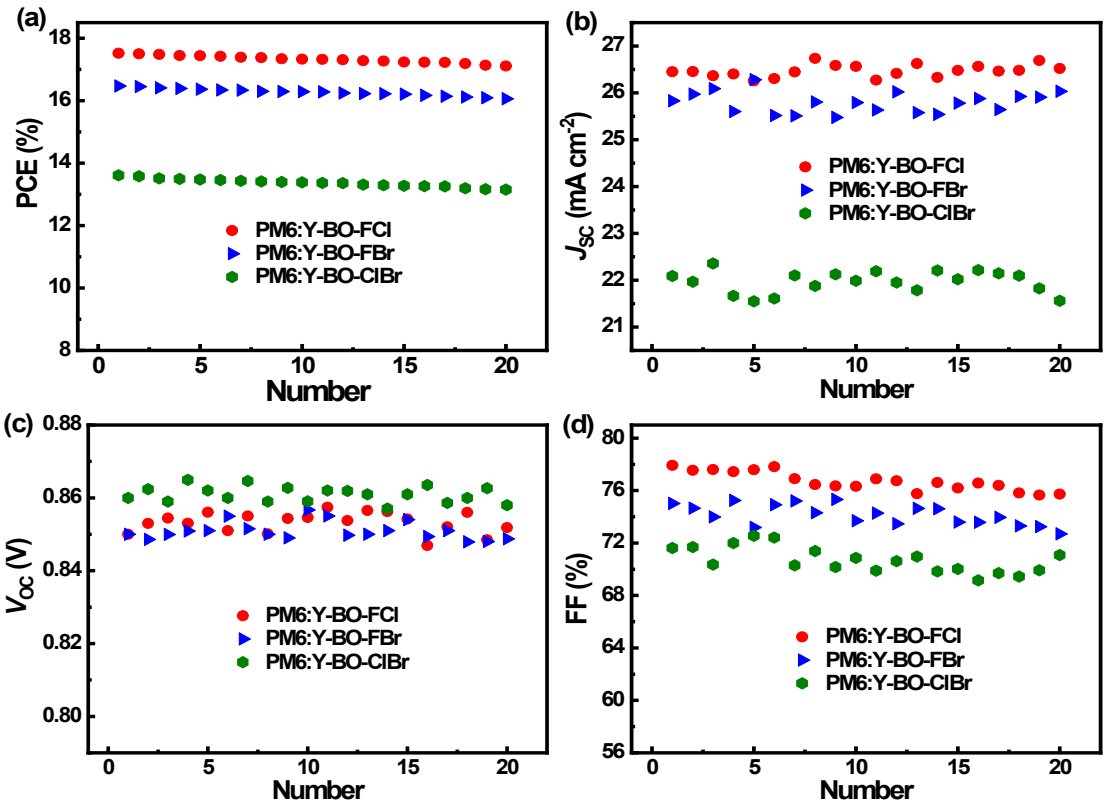

Figure S10. The distribution of photovoltaic parameters (PCE, J_{SC}, V_{OC} and FF) according to 20 cells for each kind of OSCs fabricated in different batches.

Table S3. Summary of the photovoltaic parameters for recently reported efficient binary OSCs based on hetero-halogen-modified acceptors.

Donor: Acceptor	V_{oc} [V]	J_{sc} [mA cm^{-2}]	FF [%]	PCE [%]	Reference
PM6:BTP-ClBr-1	0.854	23.66	72.2	14.56	[S3]
PM6:BTP-ClBr-2	0.845	24.97	73.6	15.54	[S3]
PM6:BTP-ClBr	0.906	23.48	79.0	16.82	[S3]
PM6:BTIC-2Cl-γCF$_3$	0.84	25.09	76.99	16.31	[S4]
PM6:BTIC-γCl-2F	0.86	24.60	72.67	15.43	[S5]

PM6:BTP-2F-ThCl	0.869	25.38	77.4	17.06	[S6]
PM6:SY1	0.871	25.41	76.0	16.83	[S7]
PM6:SY2	0.852	25.29	74.3	16.01	[S7]
PM6:BTP-S1	0.934	22.39	72.7	15.21	[S8]
BTR-Cl:BTP-2F-2Cl	0.823	22.35	71.41	13.1	[S9]
BTR-Cl:BTP-FCl-FCl	0.825	24.58	75.36	15.3	[S9]
PM7:BDSe-2(BrCl)	0.83	22.91	76.5	14.54	[S10]
PM6:Y-BO-FBr	0.85	25.83	75.02	16.47	this work
PM6:Y-BO-ClBr	0.86	22.09	71.62	13.61	this work
PM6:Y-BO-FCl	**0.85**	**26.45**	**77.92**	**17.52**	**this work**

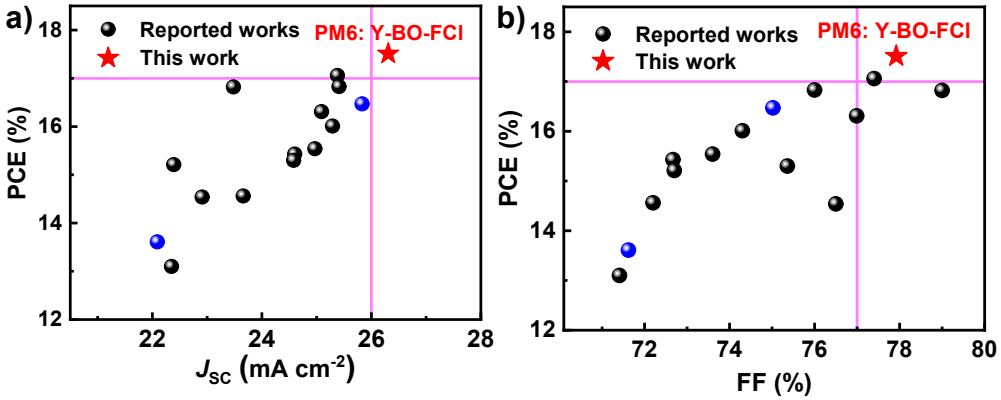

Chart S1. PCE versus FF (a) and PCE versus J_{SC} (b) in recently reported binary OSCs based on hetero-halogen-modified acceptors and compared with our **PM6**:**Y-BO-FCl** binary PSCs.

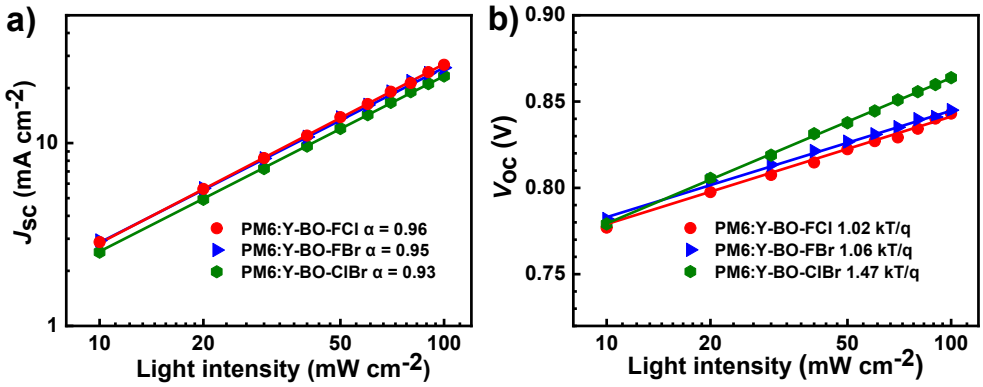

Figure S11. (a) The light-intensity dependence of the J_{SC} curves, (b) the light-intensity dependence of the V_{OC} curves of the OSCs based on **PM6:Y-BO-FCl**, **PM6:Y-BO-FBr**, and **PM6:Y-BO-ClBr**, respectively.

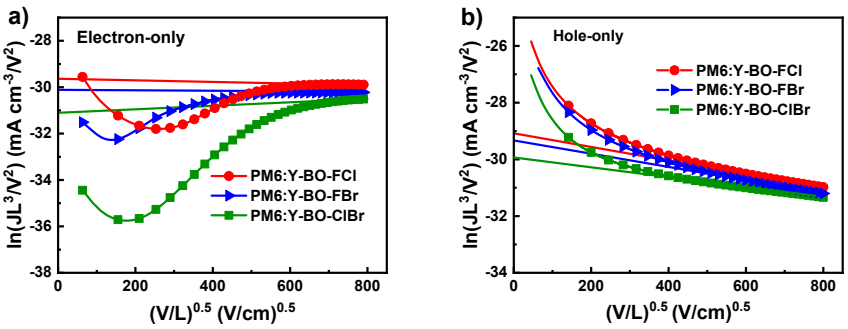

Figure S12. The $\ln(JL^3/V^2)$ vs $(V/L)^{0.5}$ curves of (a) electron-only devices and (b) hole-only devices under dark condition for these blend films by space-charge-limited current method.

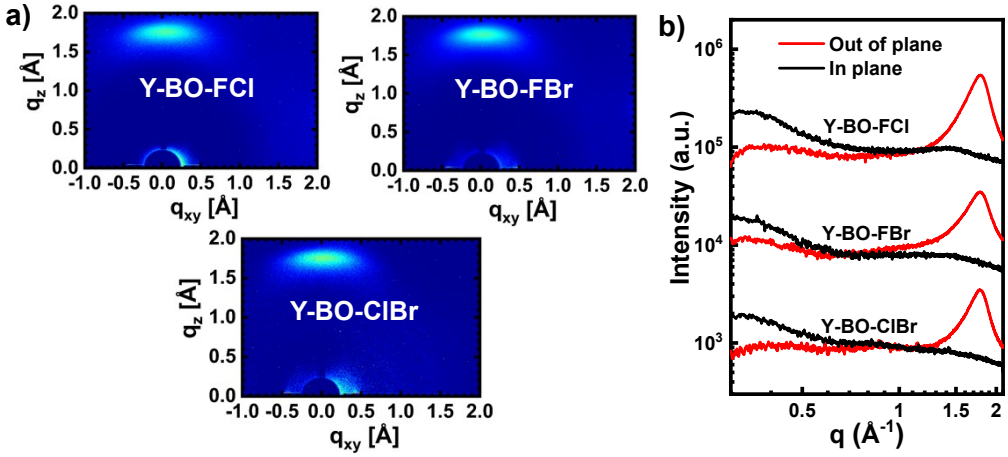

Figure S13. (a) 2D-GIXD patterns and (b) the 1D-line-cuts of GIXD for neat **Y-BO-FCl, Y-BO-FBr** and **Y-BO-ClBr** films, respectively.

4. ^{1}H NMR, ^{13}C NMR, and HR-FTMS, MALDI-TOF-MS, and IR spectrum of compounds

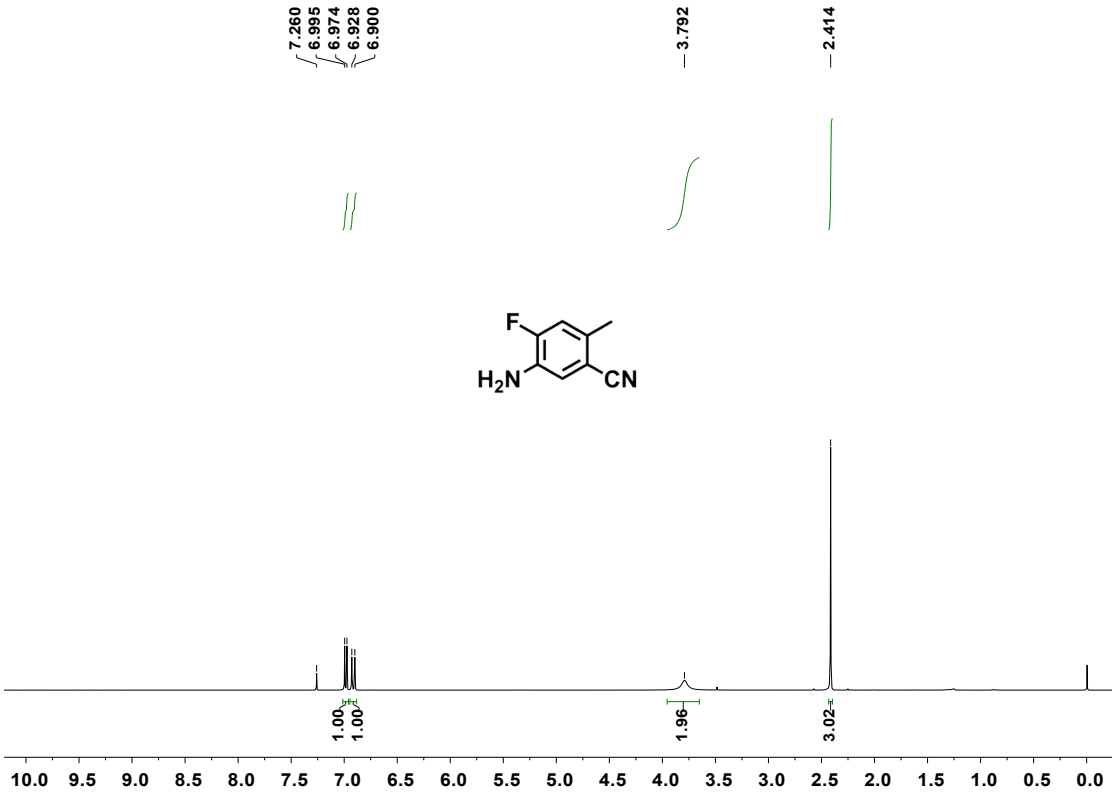

Figure S14. ^{1}H NMR spectrum for compound **1**

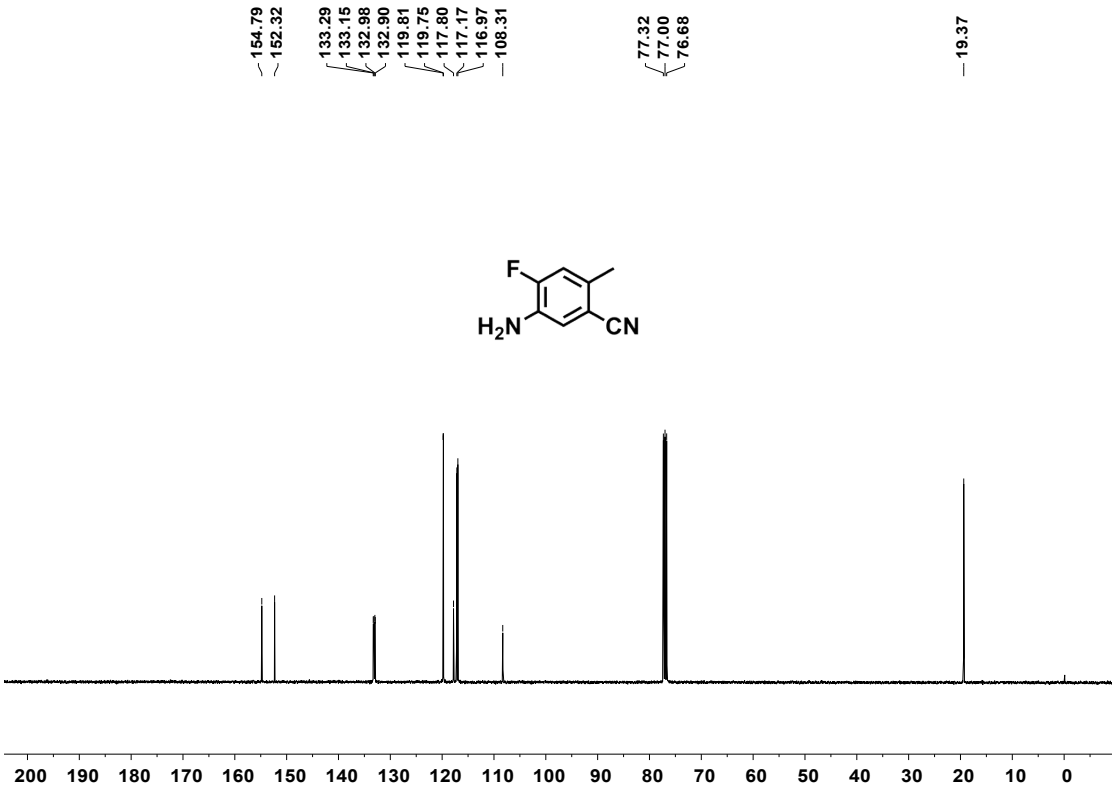

Figure S15. ^{13}C NMR spectrum for compound **1**

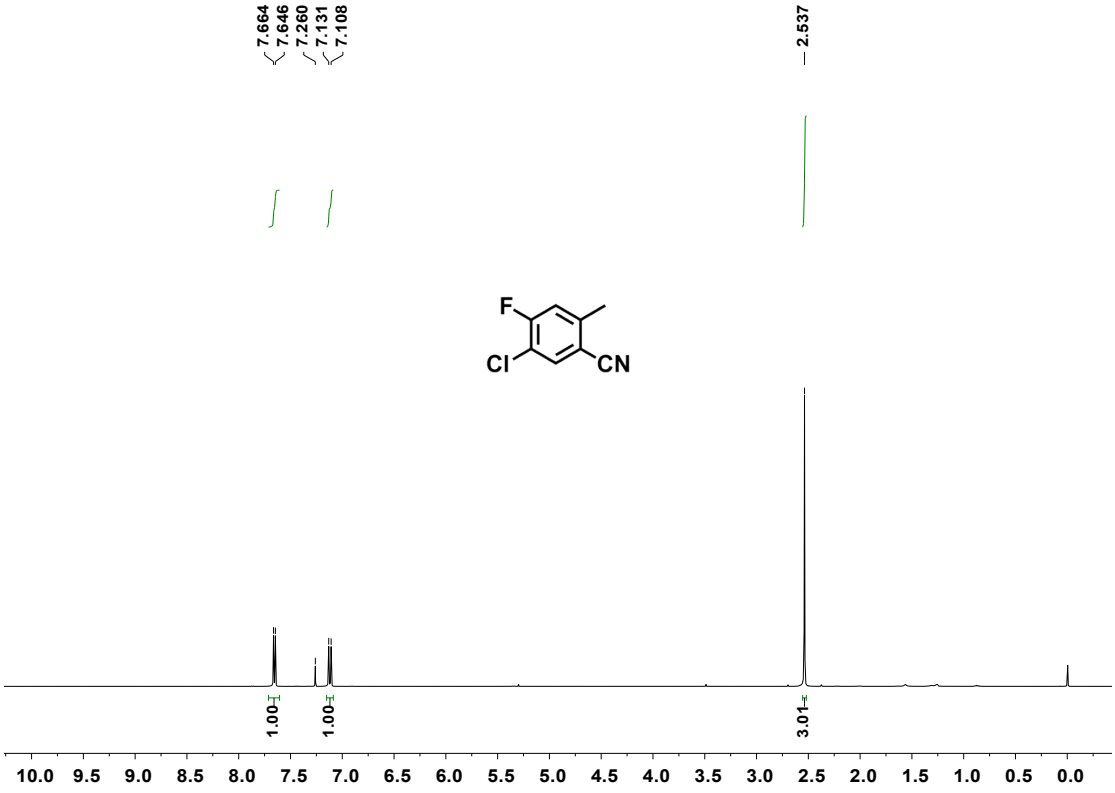

Figure S16. ^{1}H NMR spectrum for compound **2a**

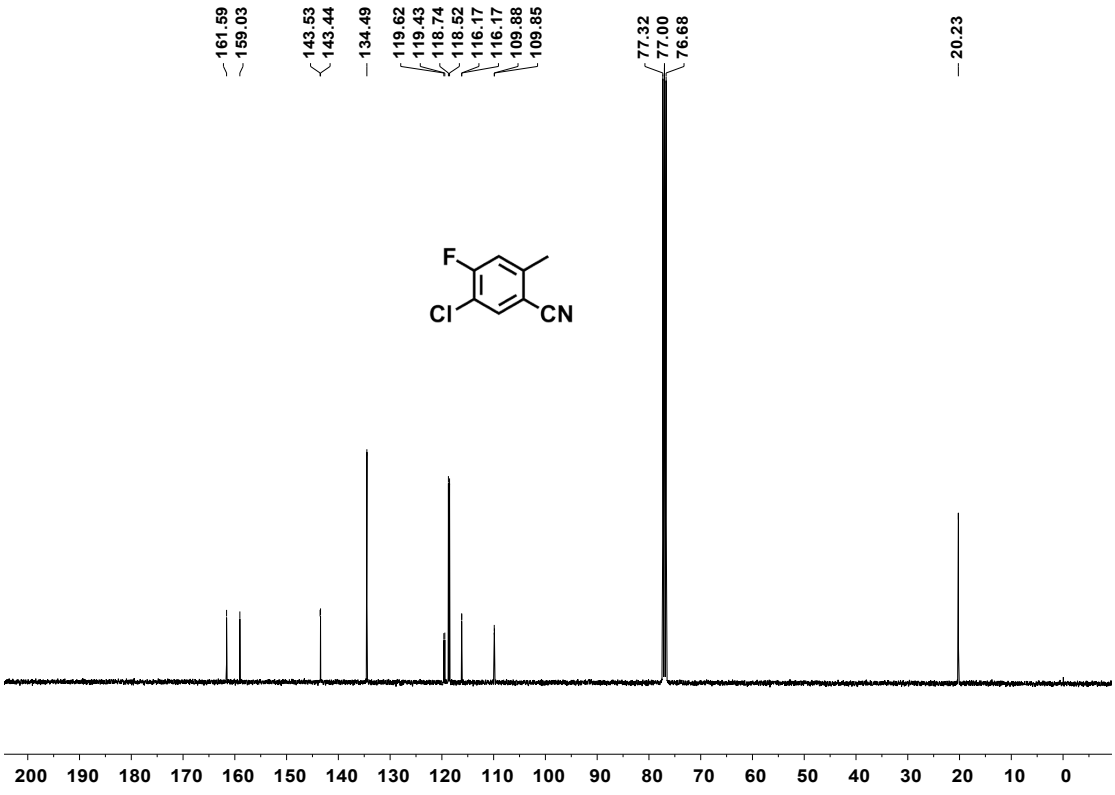

Figure S17. ^{13}C NMR spectrum for compound **2a**

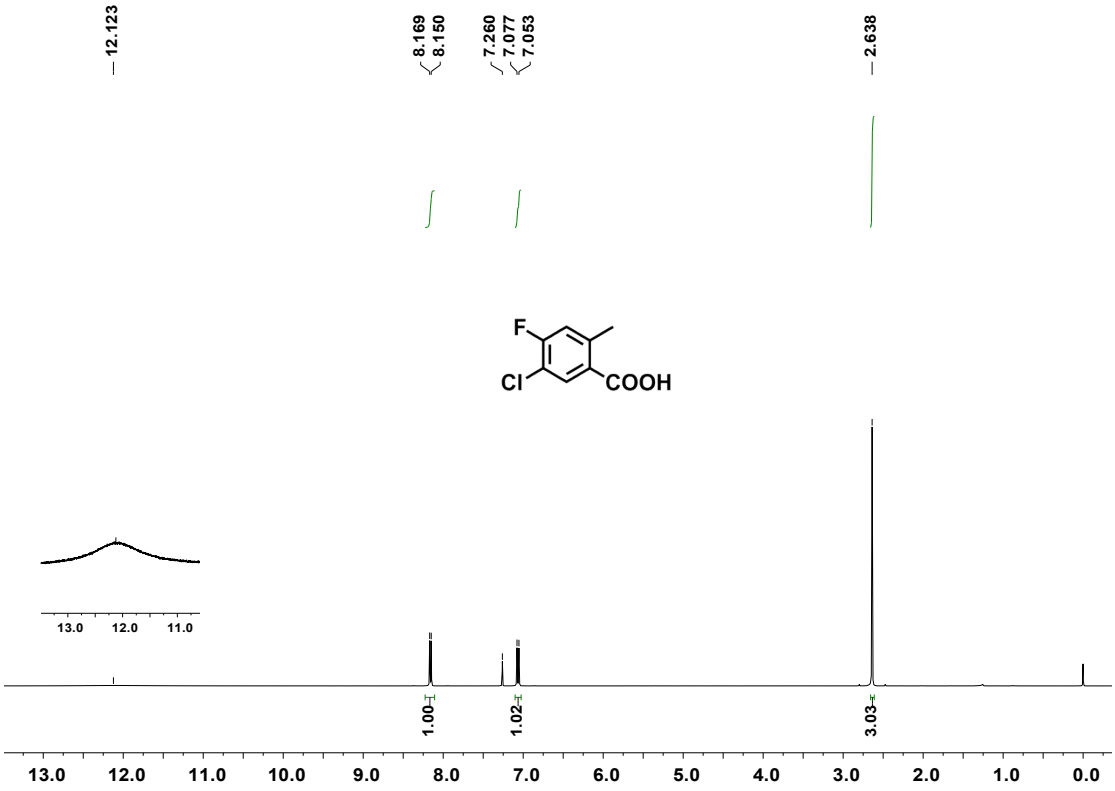

Figure S18. ^{1}H NMR spectrum for compound **3a**

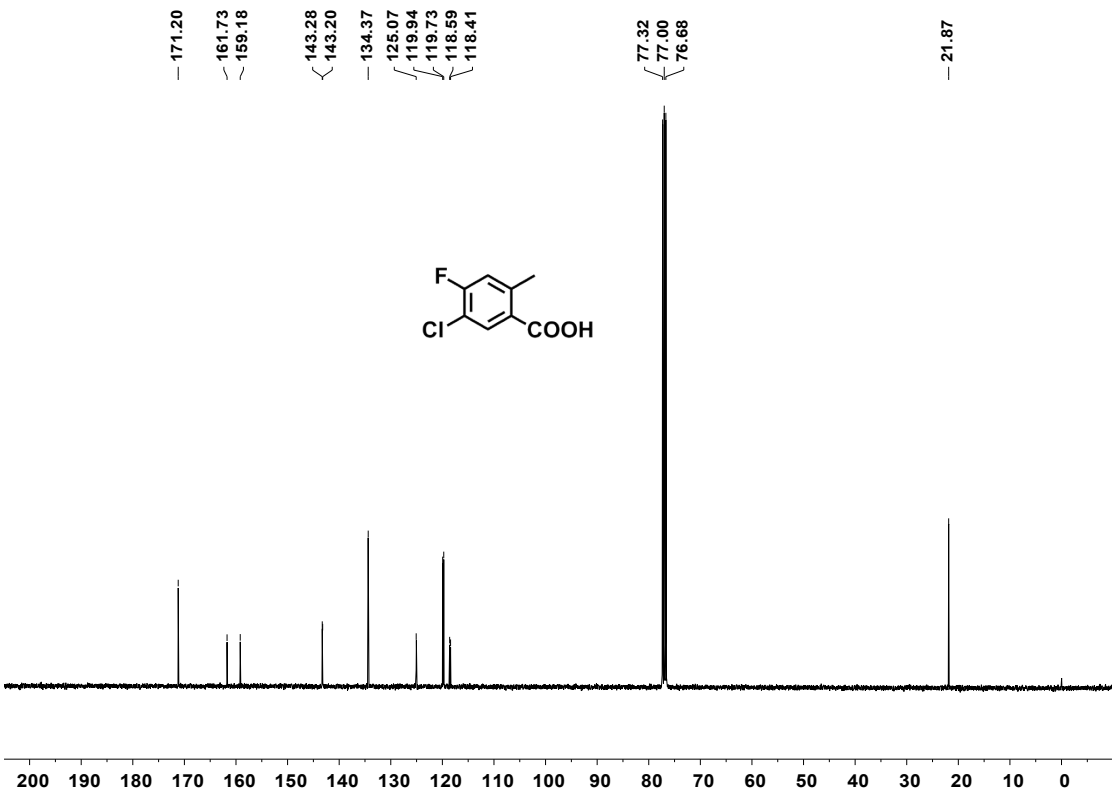

Figure S19. ^{13}C NMR spectrum for compound **3a**

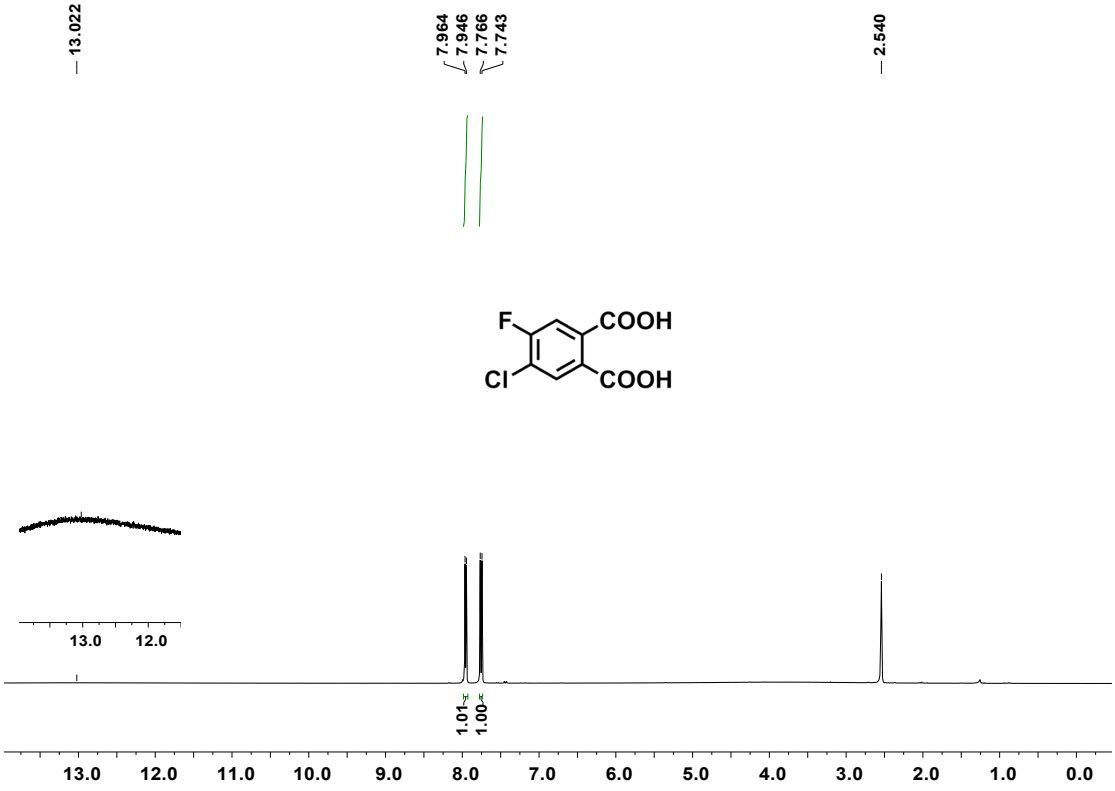

Figure S20. ^{1}H NMR spectrum for compound **4a** in d_6-DMSO

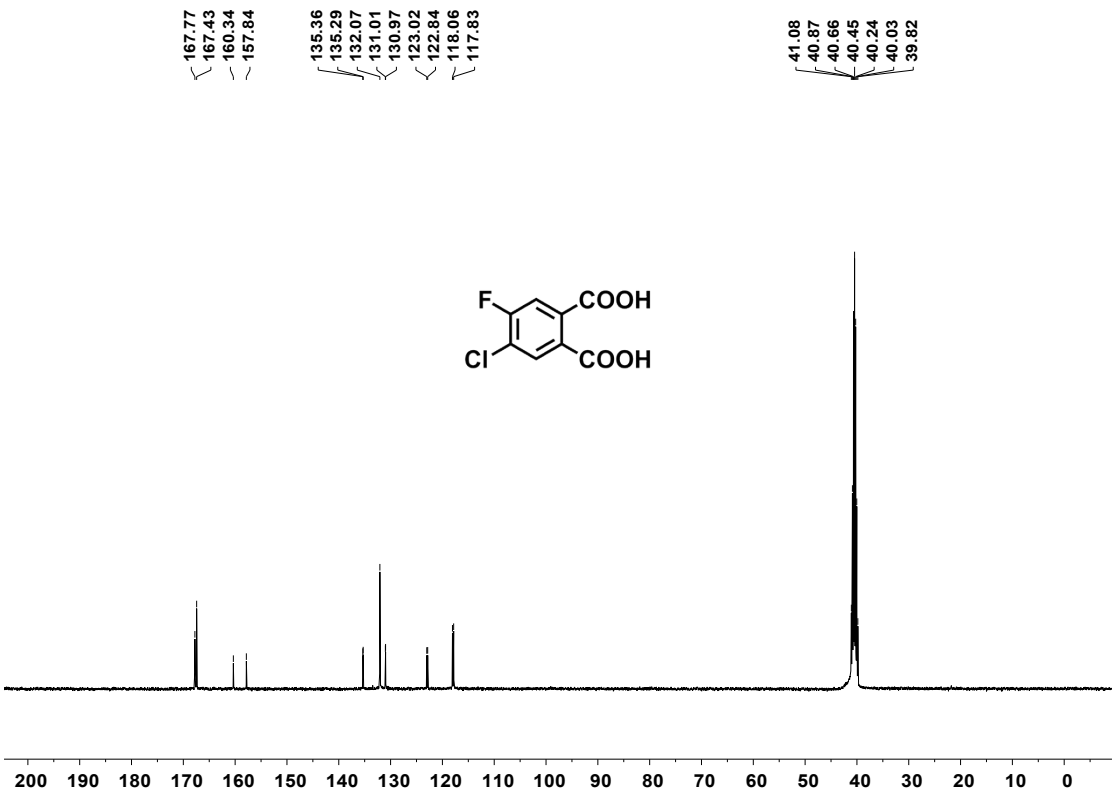

Figure S21. ^{13}C NMR spectrum for compound **4a** in d_6-DMSO

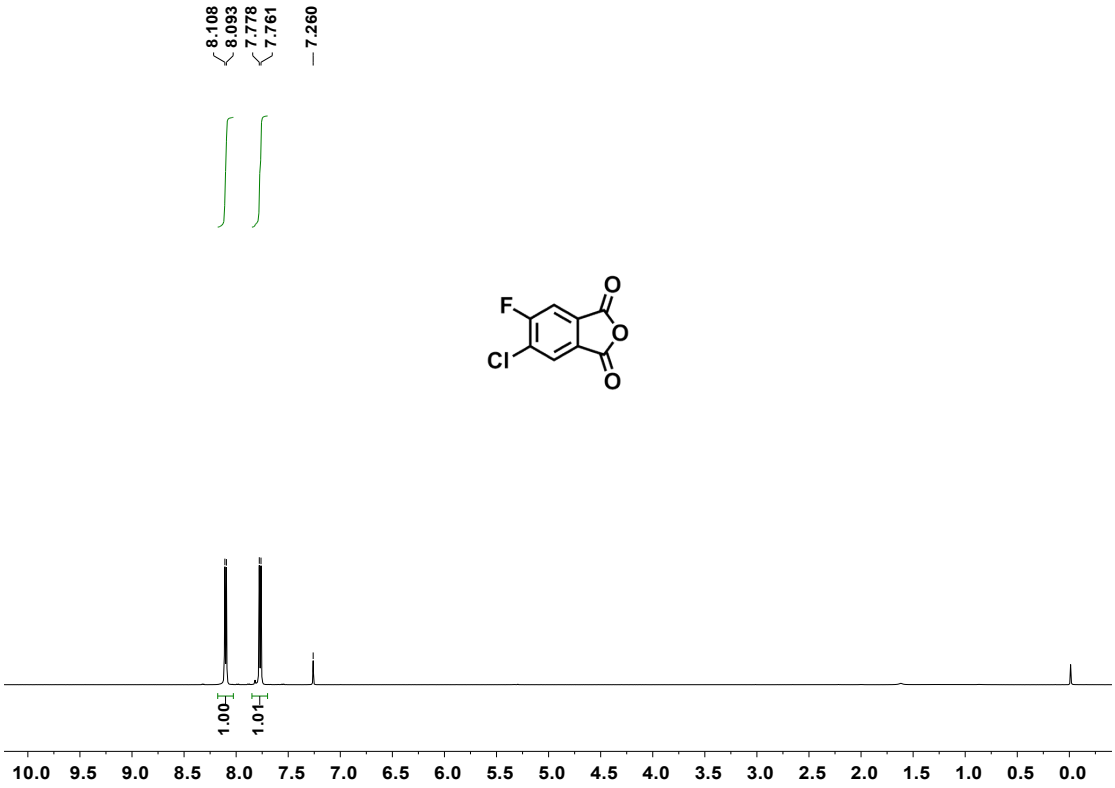

Figure S22. ^{1}H NMR spectrum for compound **5a**

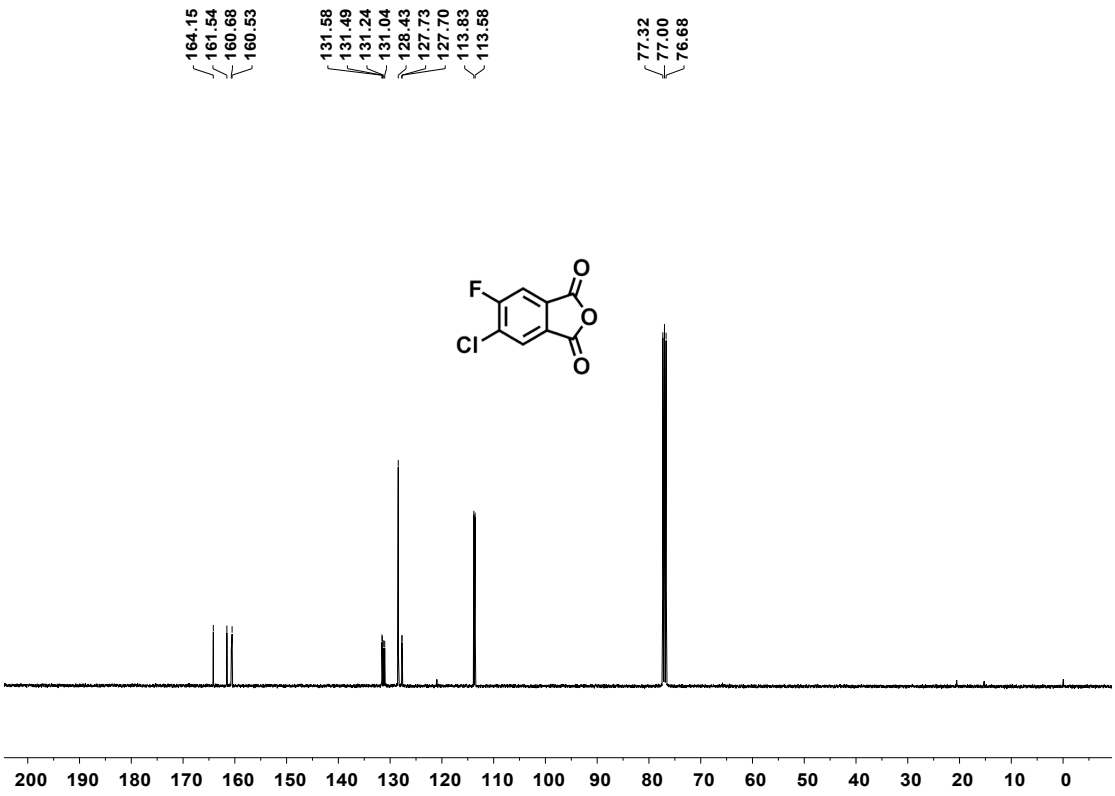

Figure S23. ^{13}C NMR spectrum for compound **5a**

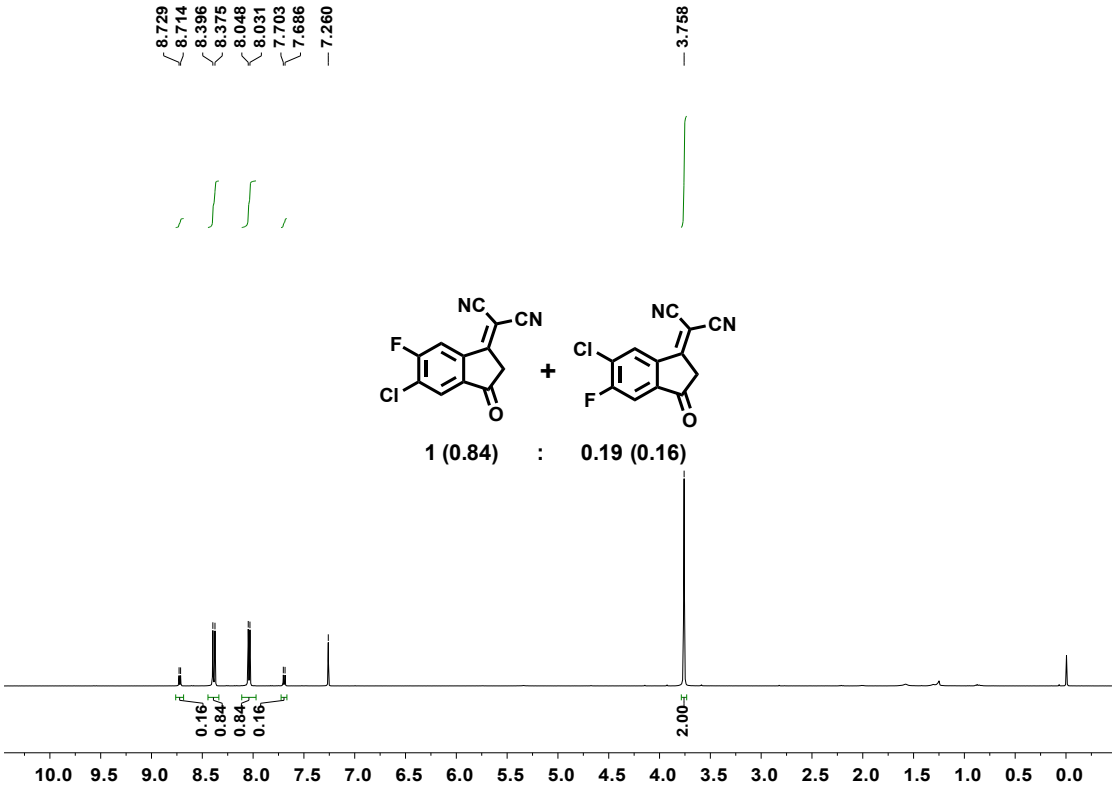

Figure S24. ^{1}H NMR spectrum for **FCl-IC**

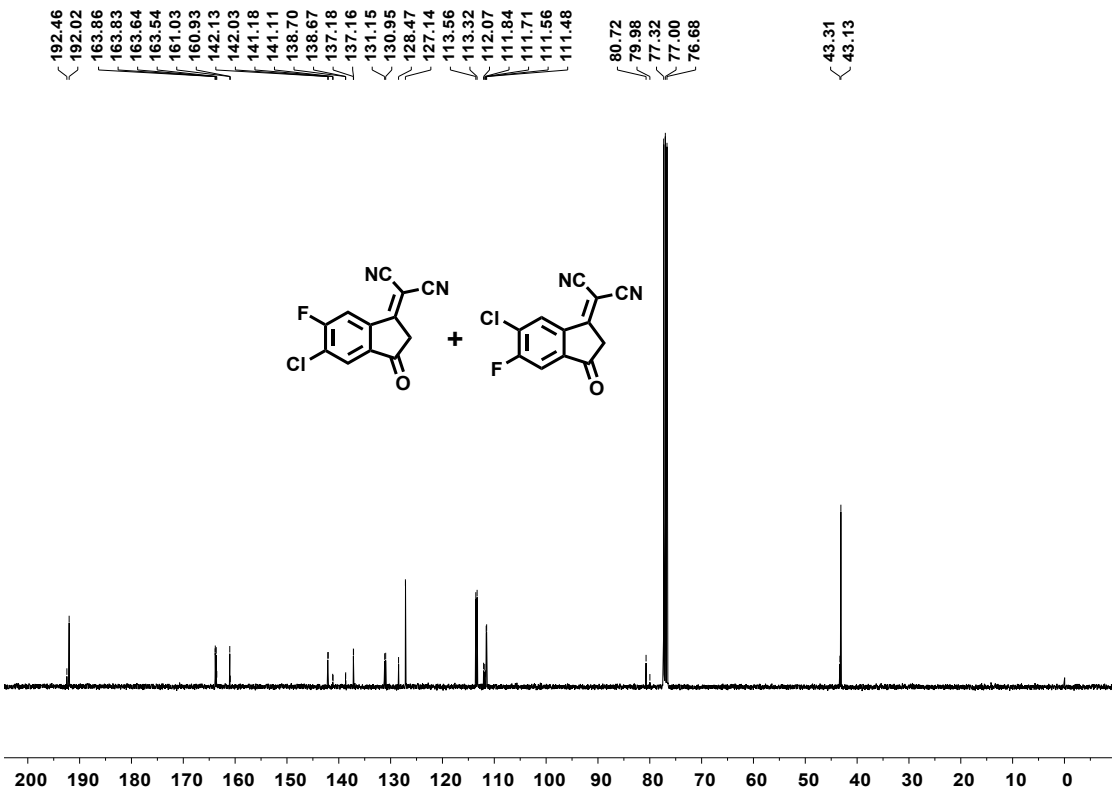

Figure S25. ^{13}C NMR spectrum for **FCl-IC**

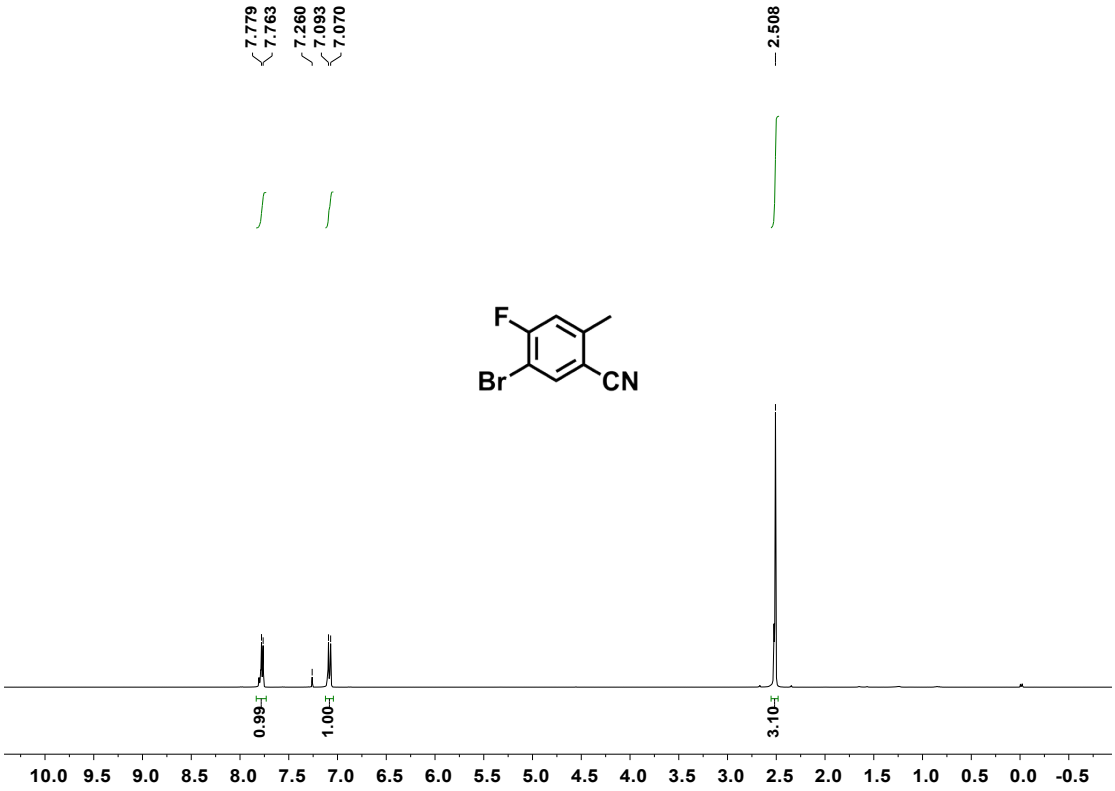

Figure S26. ^{1}H NMR spectrum for compound **2b**

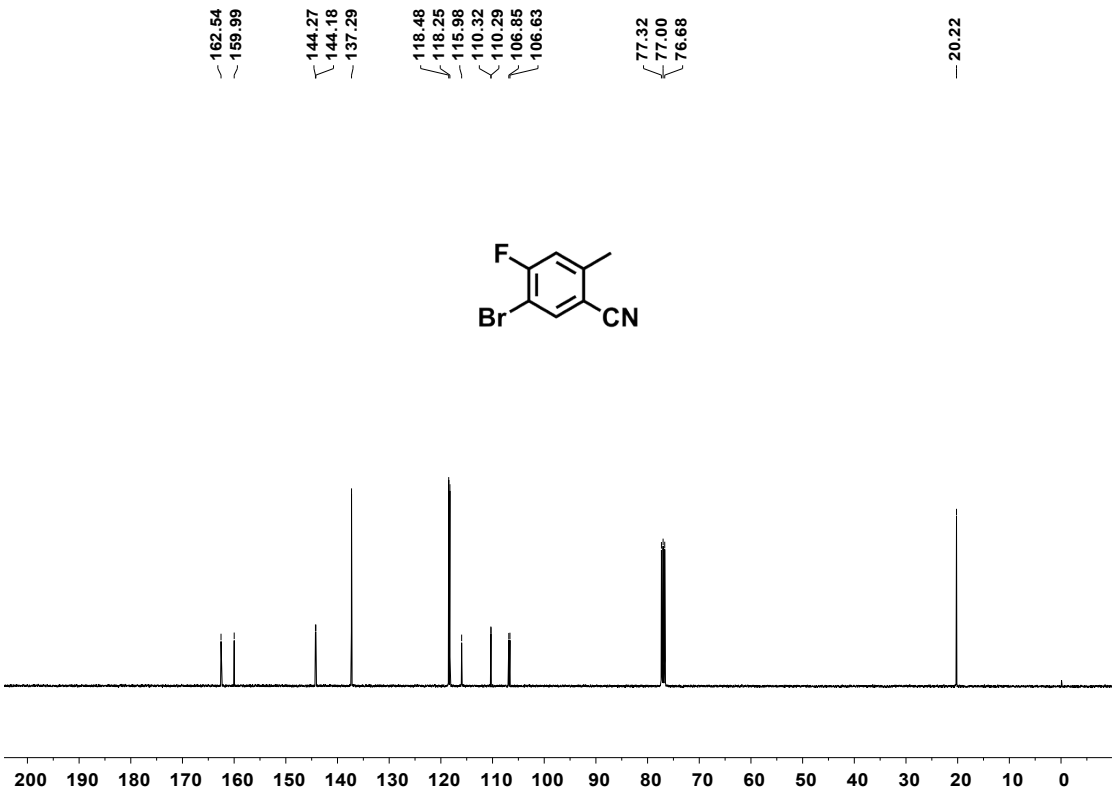

Figure S27. ^{13}C NMR spectrum for compound **2b**

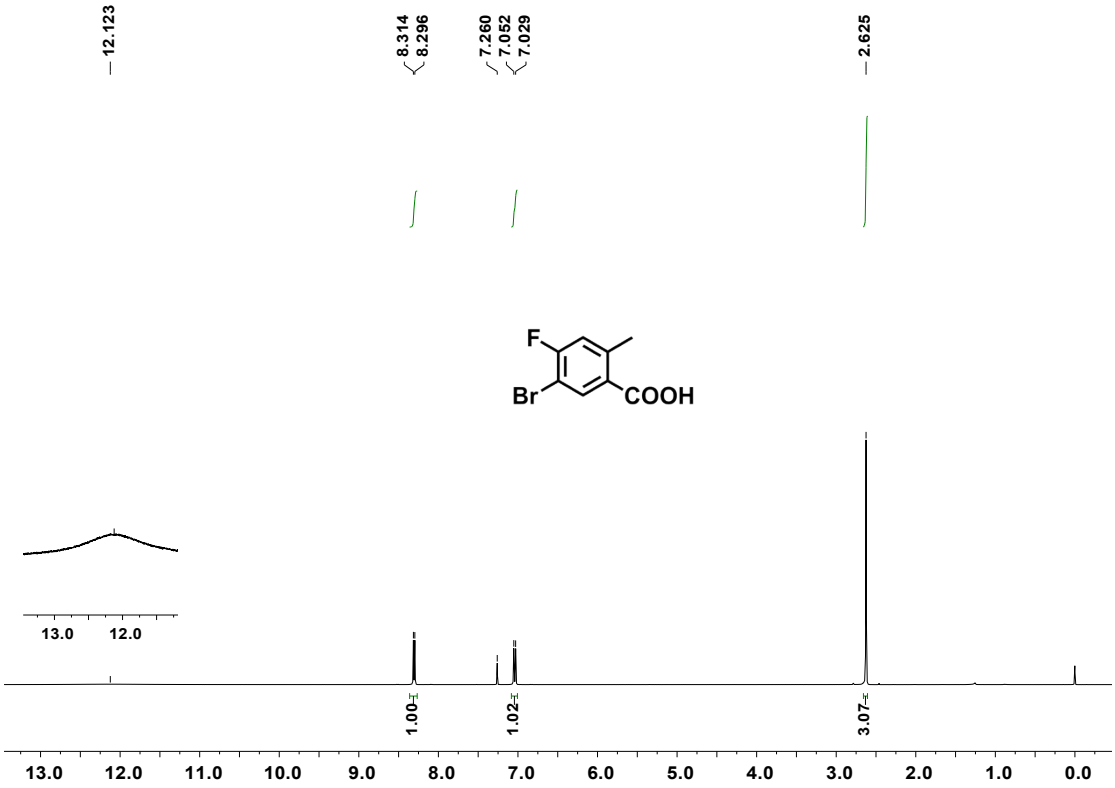

Figure S28. ^{1}H NMR spectrum for compound **3b**

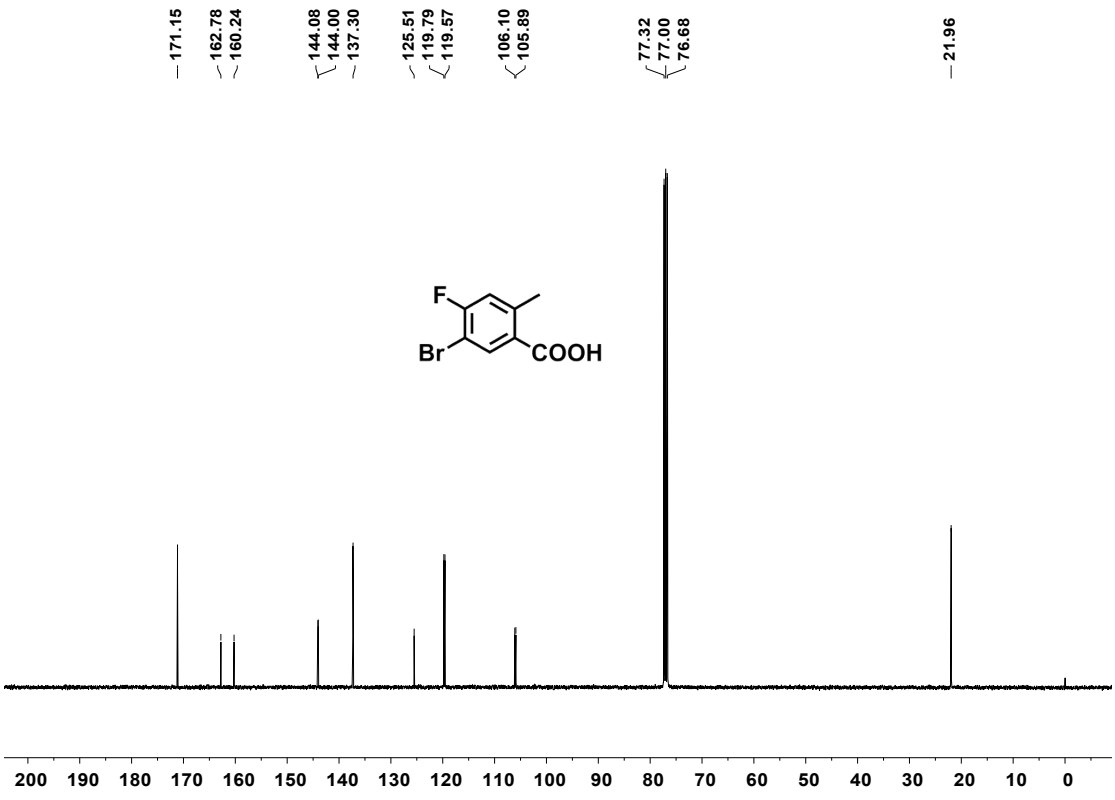

Figure S29. ^{13}C NMR spectrum for compound **3b**

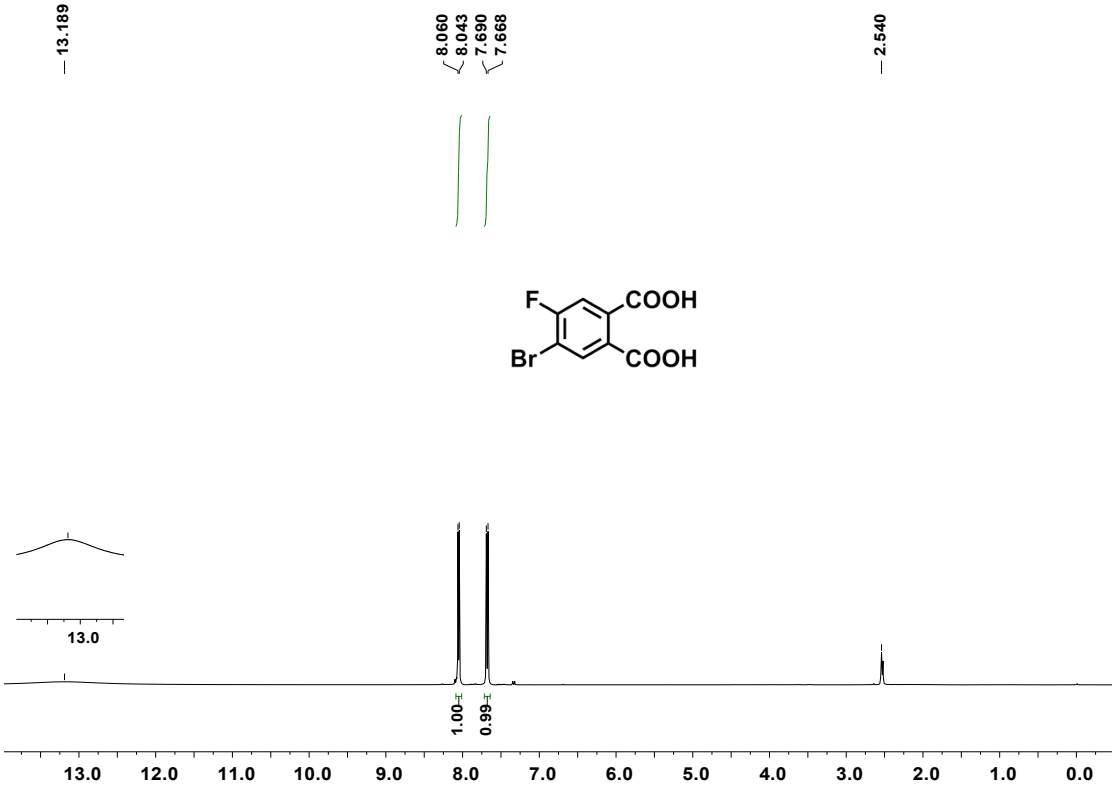

Figure S30. ^{1}H NMR spectrum for compound **4b** in d_6-DMSO

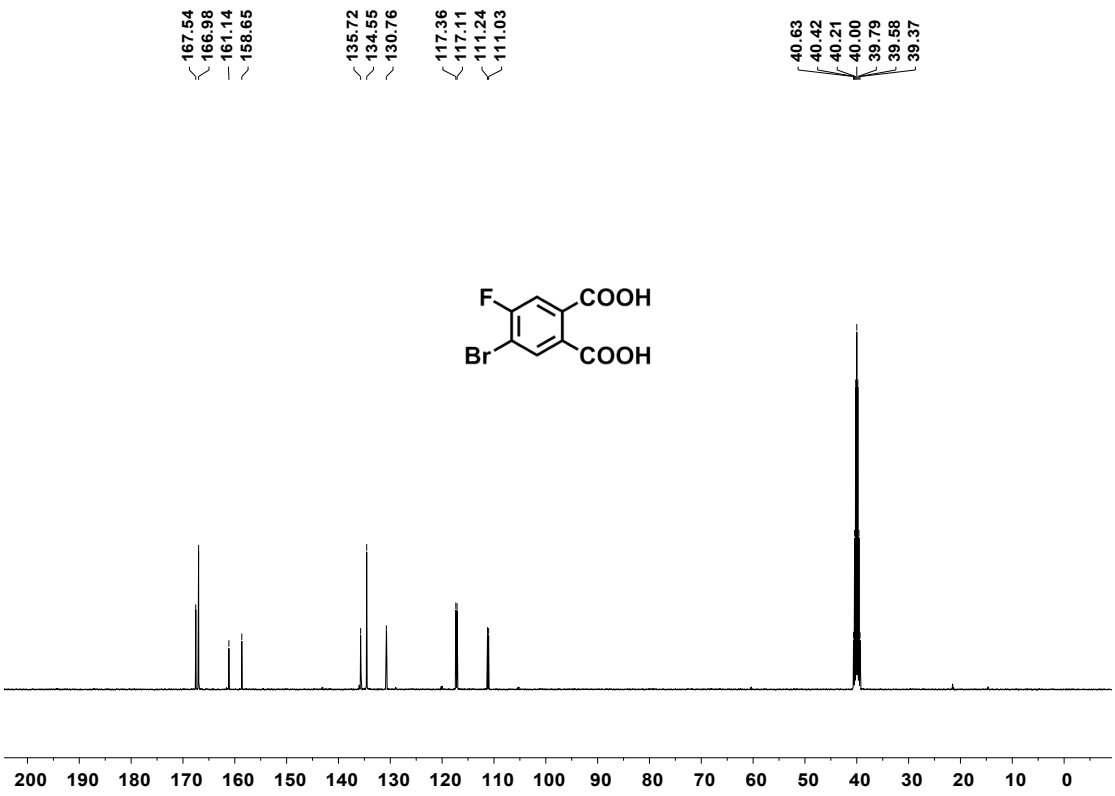

Figure S31. ^{13}C NMR spectrum for compound **4b** in d_6-DMSO

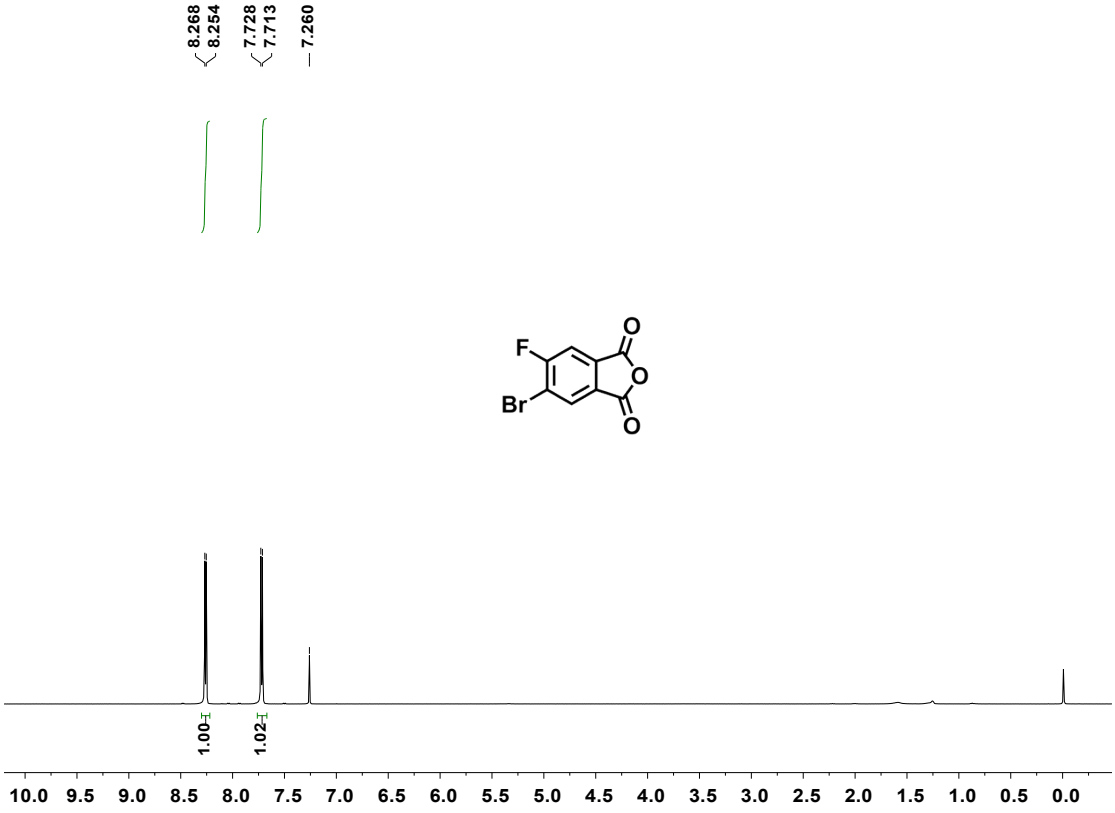

Figure S32. ^{1}H NMR spectrum for compound **5b**

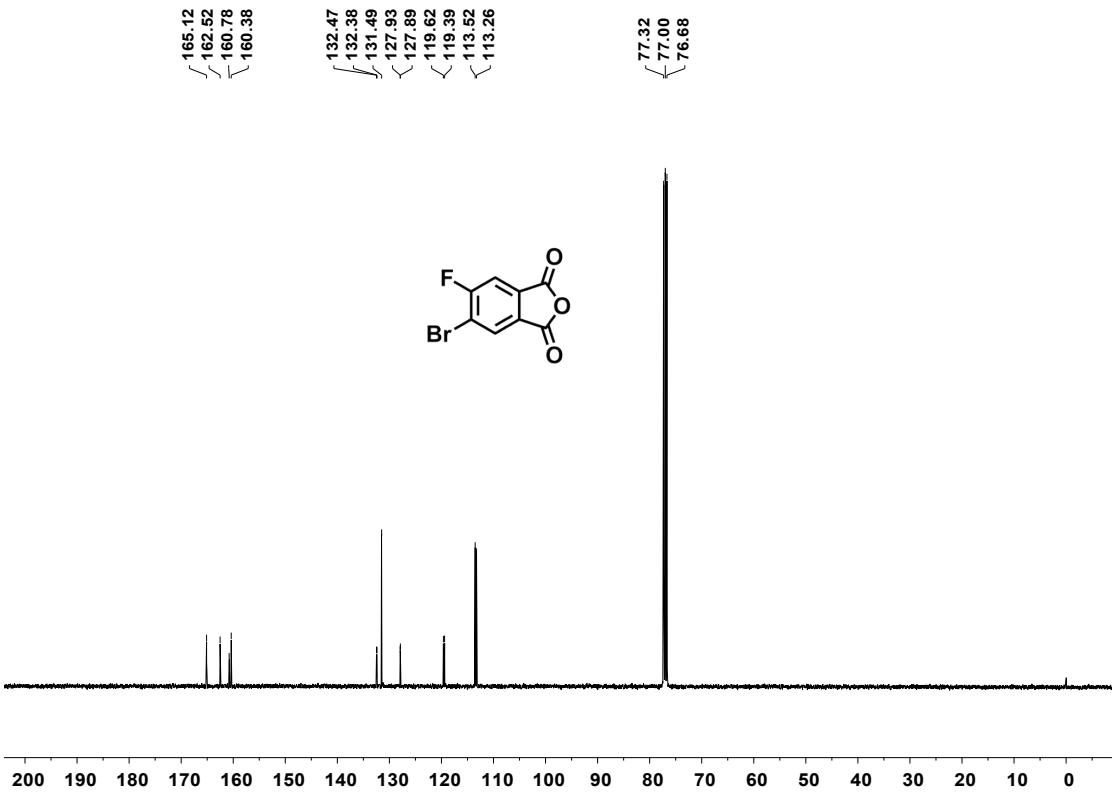

Figure S33. ^{13}C NMR spectrum for compound **5b**

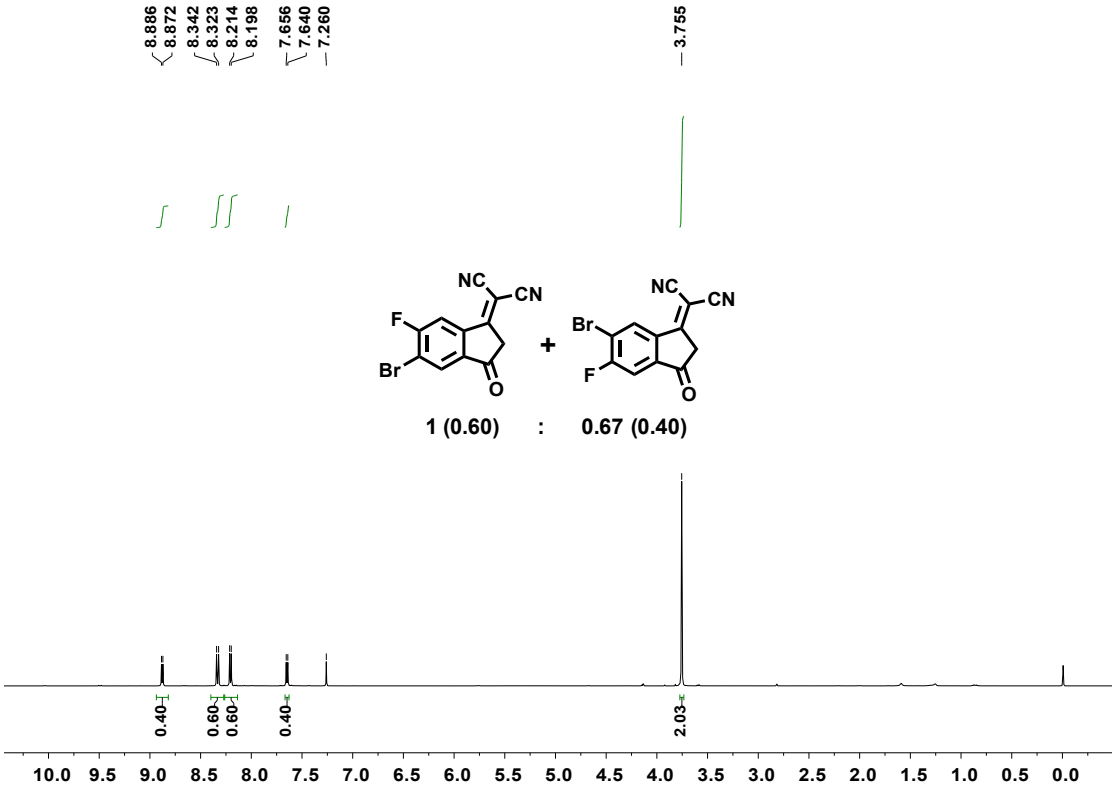

Figure S34. ^{1}H NMR spectrum for **FBr-IC**

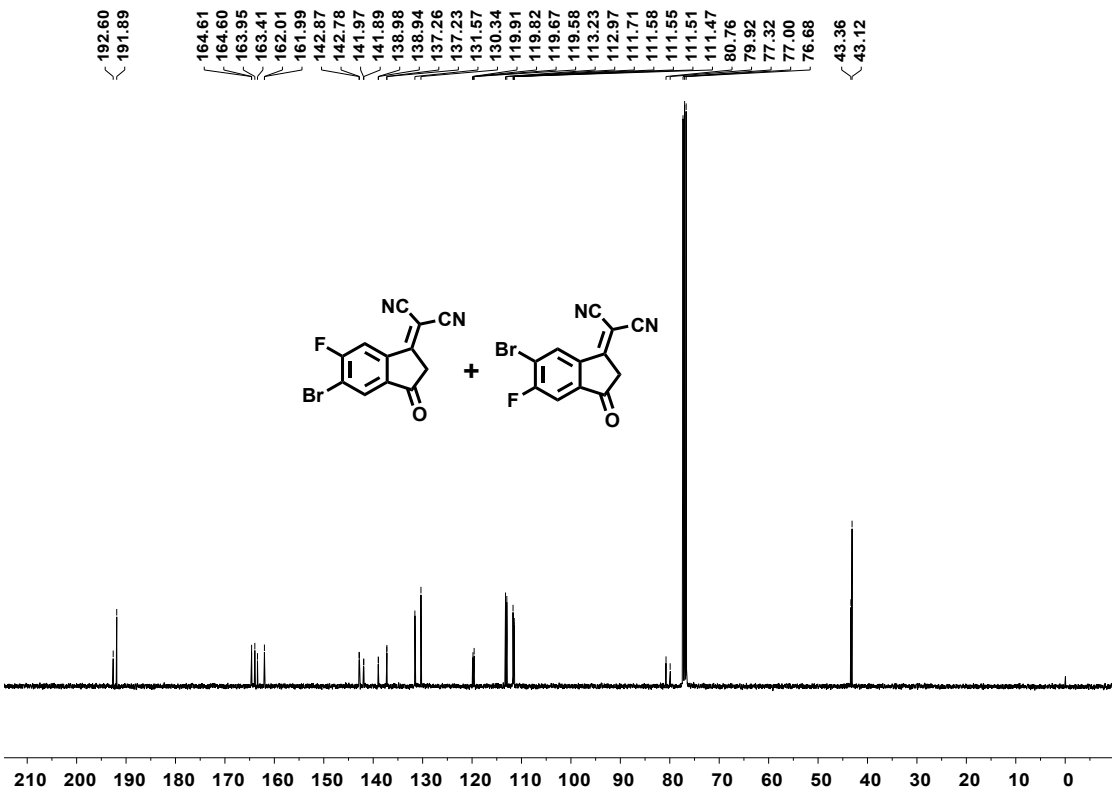

Figure S35. ^{13}C NMR spectrum for **FBr-IC**

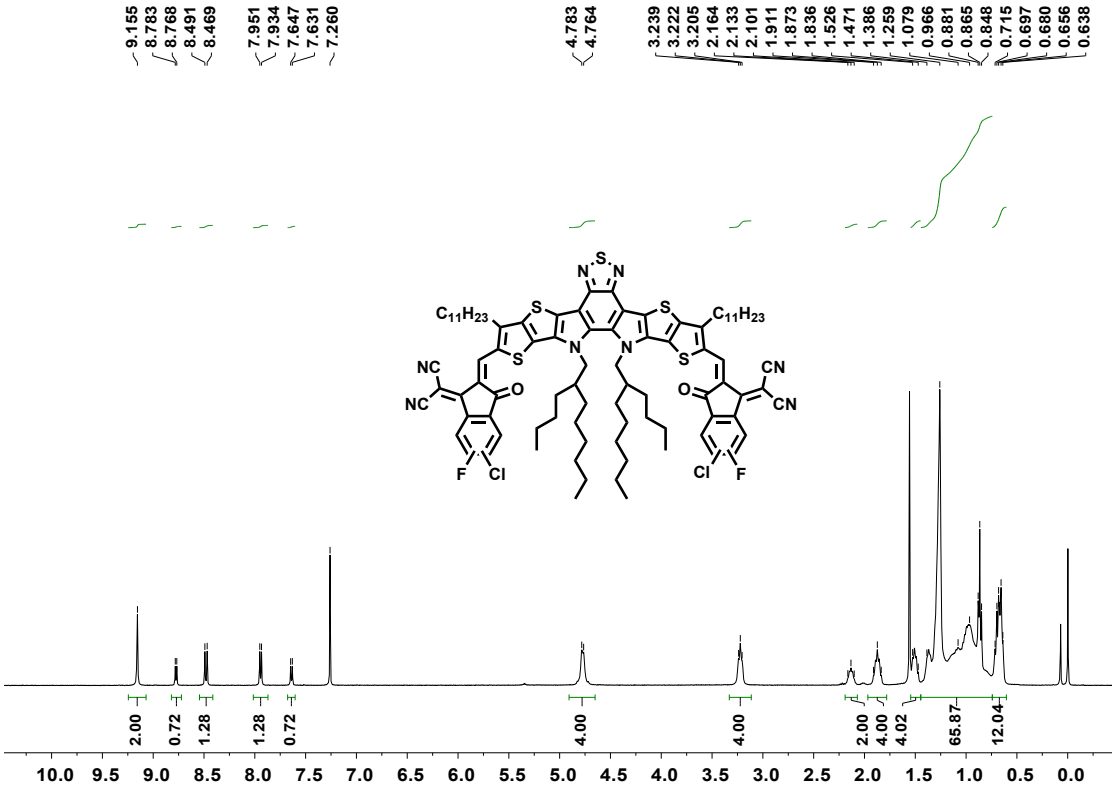

Figure S36. ^{1}H NMR spectrum for **Y-BO-FCl**

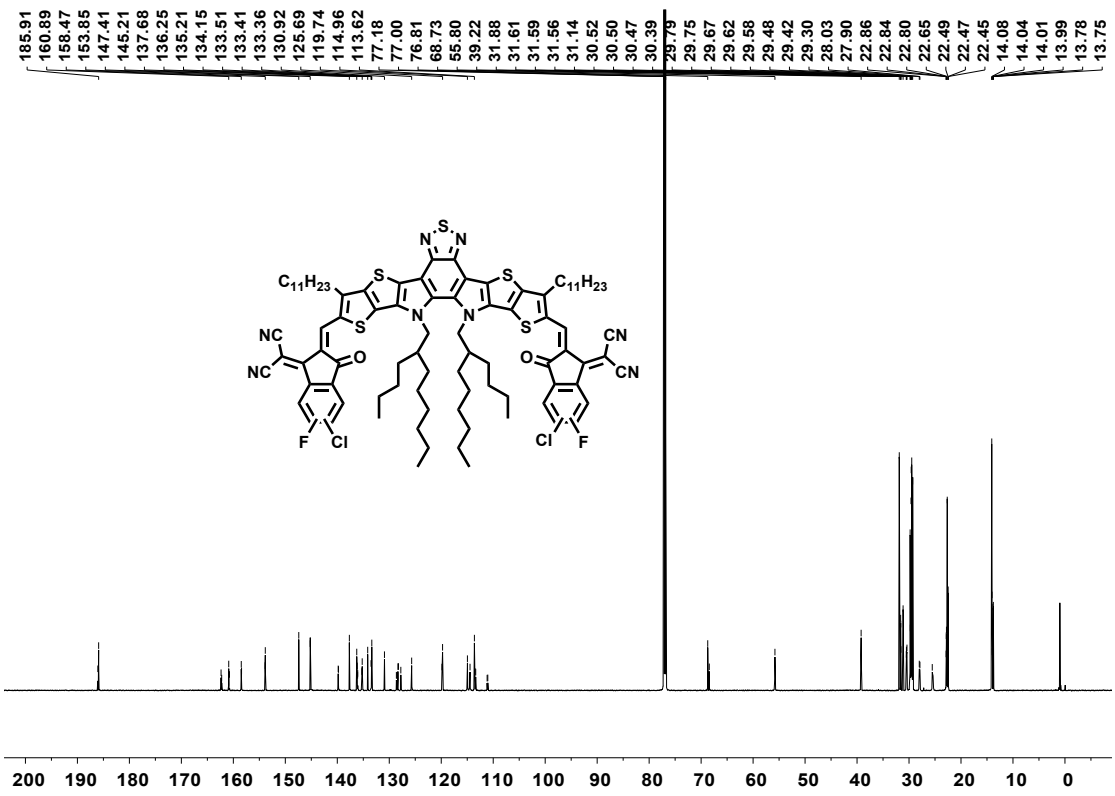

Figure S37. ^{13}C NMR spectrum for **Y-BO-FCl**

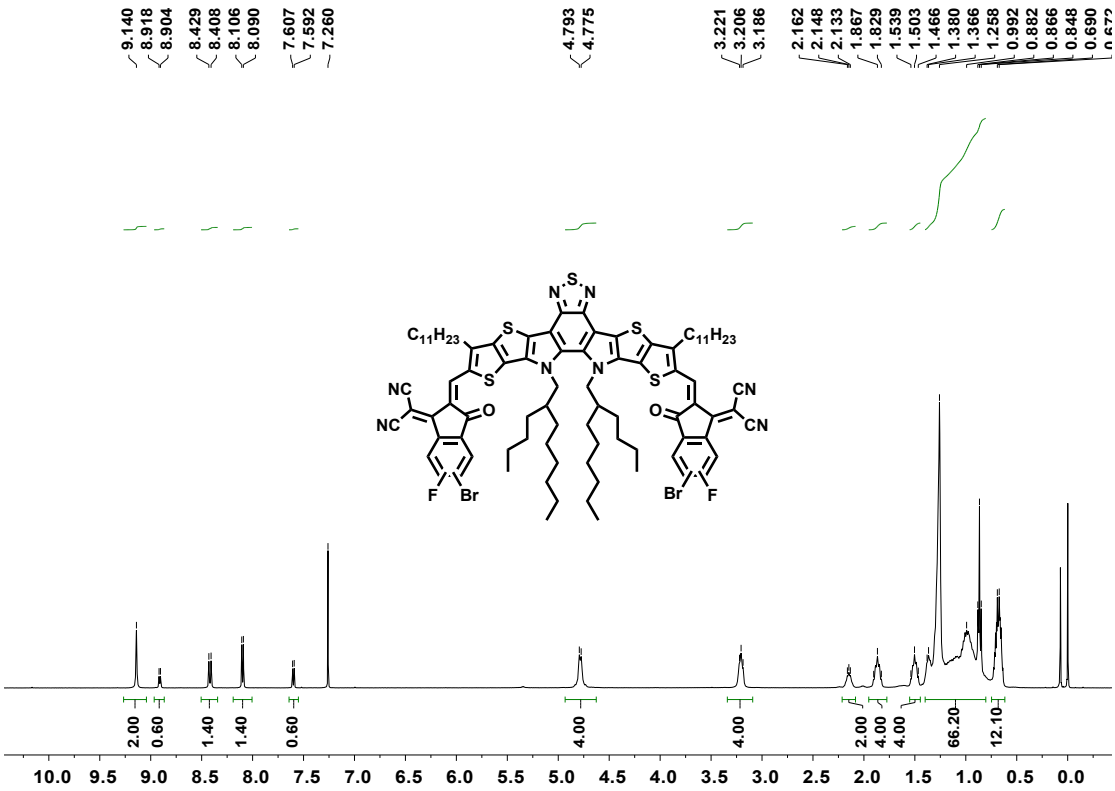

Figure S38. ^{1}H NMR spectrum for **Y-BO-FBr**

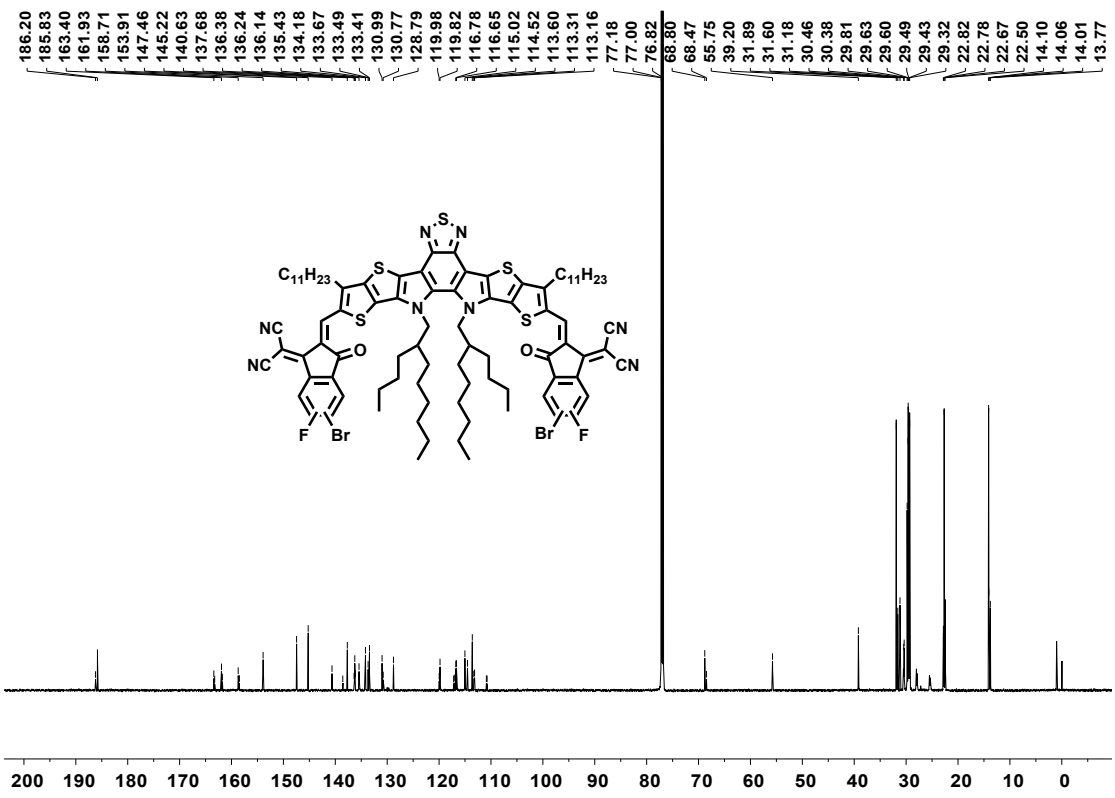

Figure S39. ^{13}C NMR spectrum for **Y-BO-FBr**

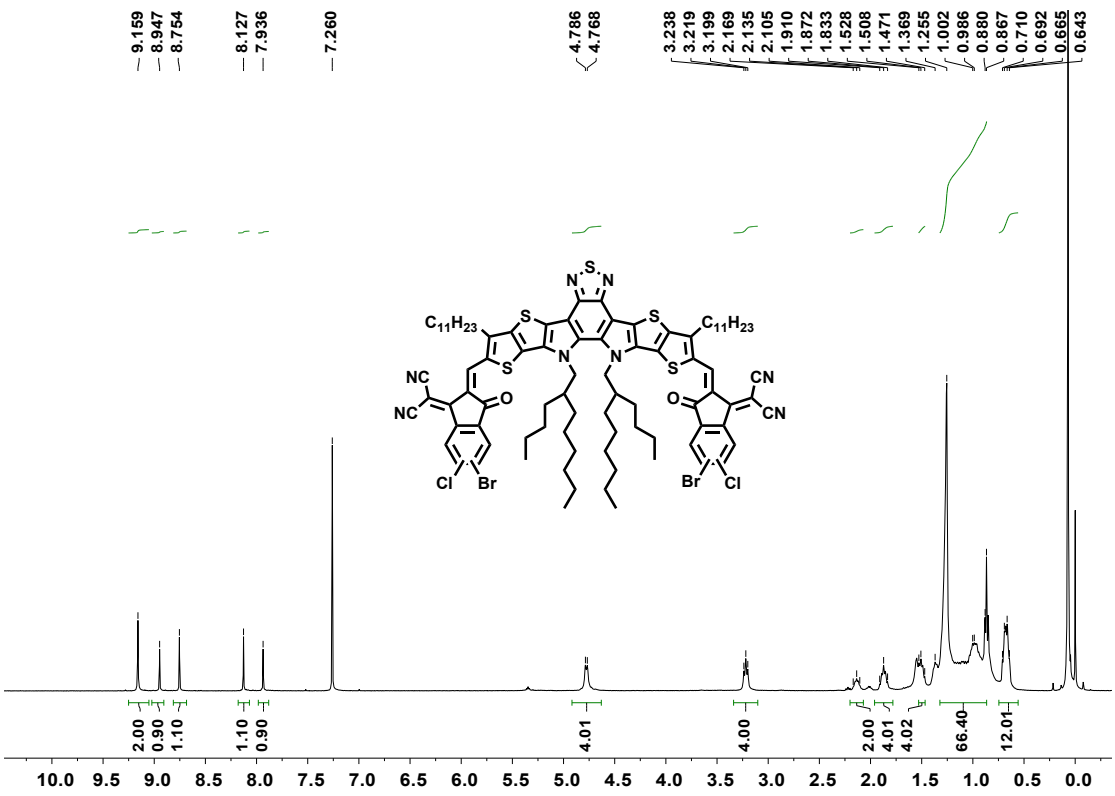

Figure S40. ^{1}H NMR spectrum for **Y-BO-ClBr**

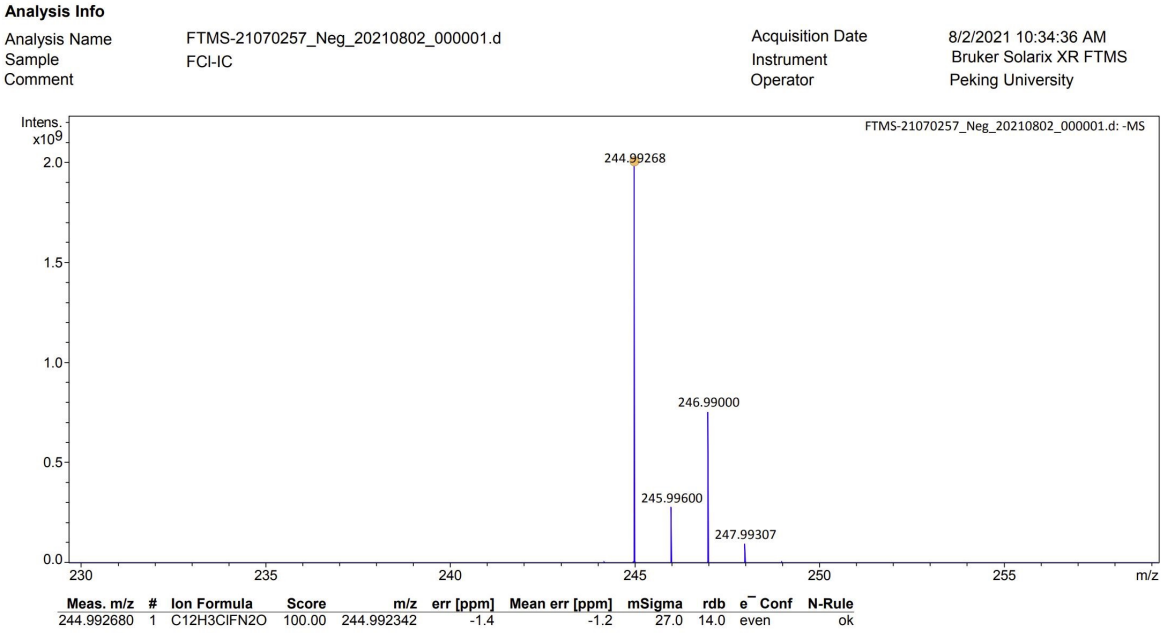

Figure S41. HR -FT-MS spectrum of **FCl-IC**

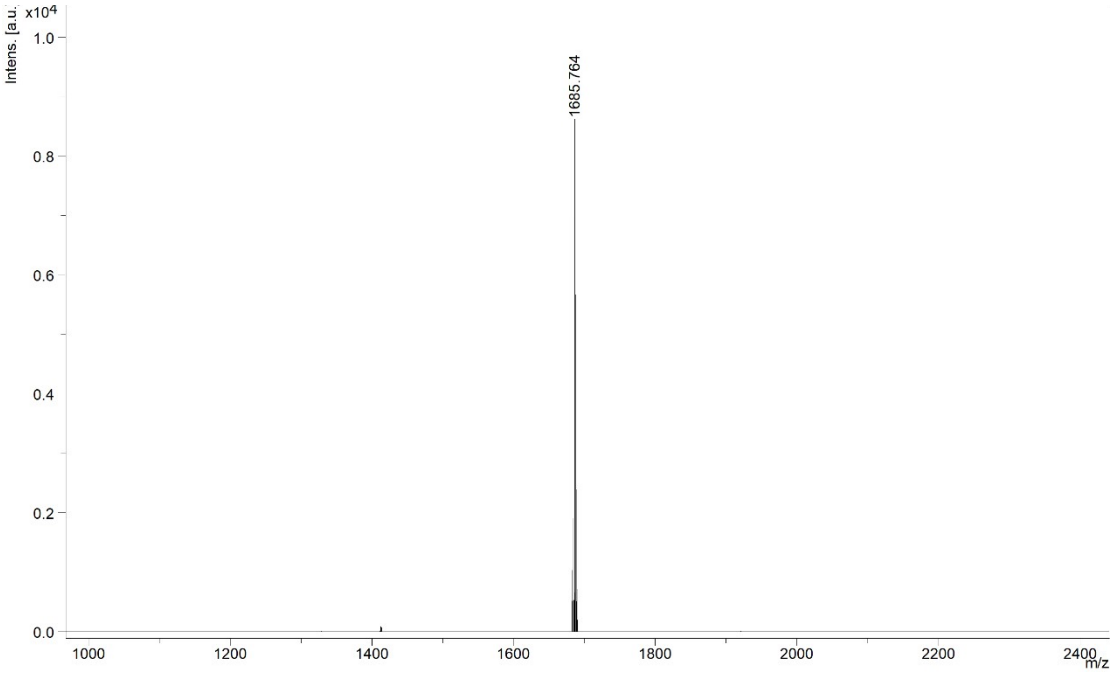

Figure S42. MALDI-TOF mass spectrum of **Y-BO-FCl**

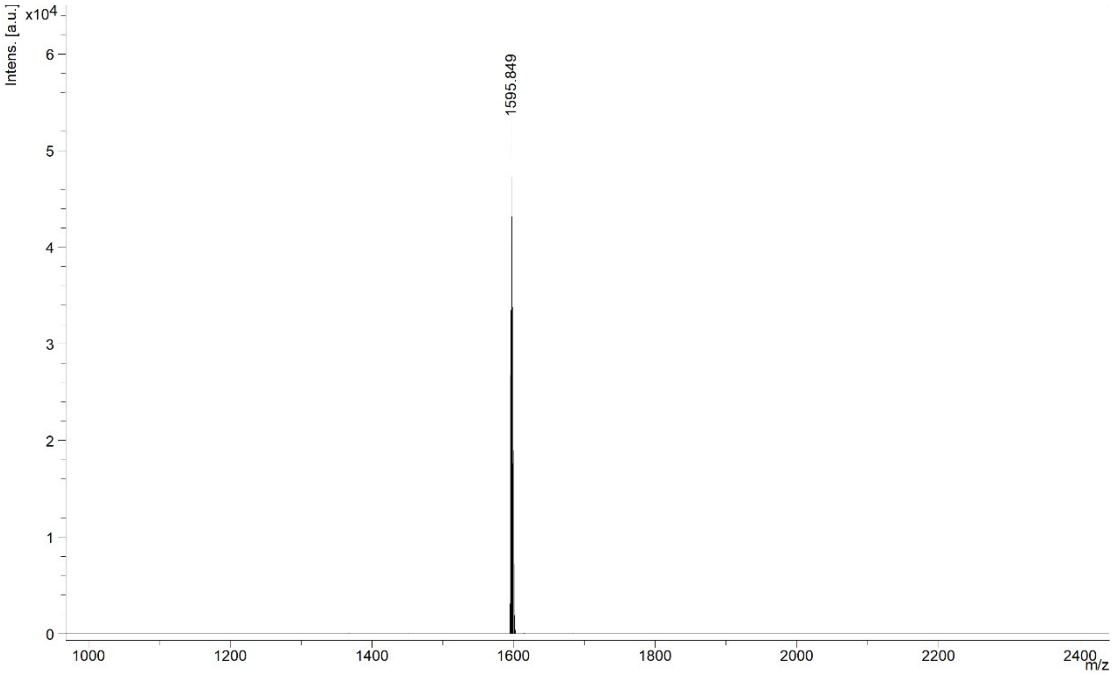

Figure S43. MALDI-TOF mass spectrum of **Y-BO-FBr**

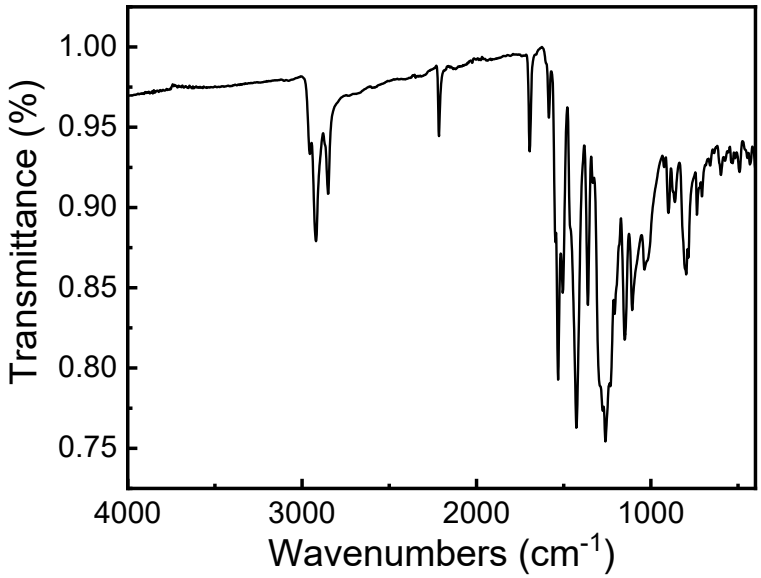

Figure S44. IR spectrum of **Y-BO-FCl**

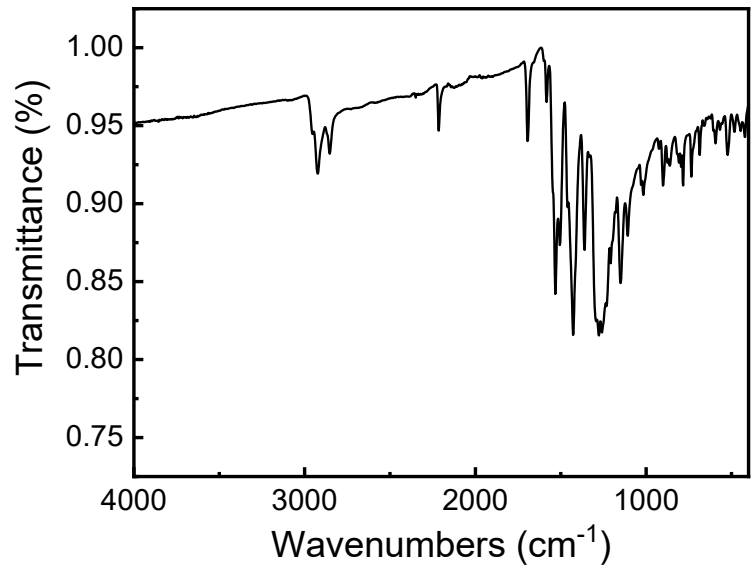

Figure S45. IR spectrum of **Y-BO-FBr**

5. References

[S1]R. A. Hartz, V. T. Ahuja, M. Rafalski, W. D. Schmitz, A. B. Brenner, D. J. Denhart, J. L. Ditta, J. A. Deskus, E. W. Yue, A. G. Arvanitis, S. Lelas, Y. W. Li, T. F. Molski, H. Wong, J. E. Grace, K. A. Lentz, J. Li, N. J. Lodge, R. Zaczek, A. P. Combs, R. E. Olson, R. J. Mattson, J. J. Bronson, J. E. Macor, *J. Med. Chem.* 2009, **52**, 4161-4172.

[S2]F. Peng, K. An, W. Zhong, Z. Li, L. Ying, N. Li, Z. Huang, C. Zhu, B. Fan, F. Huang and Y. Cao, *ACS Energy Lett.*, 2020, **5**, 3702-3707.

[S3]Z. Luo, R. Ma, Z. Chen, Y. Xiao, G. Zhang, T. Liu, R. Sun, Q. Zhan, Y. Zou, C. Zhong, Y. Chen, H. Sun, G. Chai, K. Chen, X. Guo, J. Min, X. Lu, C. Yang, H. Yan, *Adv. Energy*

Mater. 2020, **10**, 2002649.
[S4]H. Chen, H. Lai, Z. Chen, Y. Zhu, H. Wang, L. Han, Y. Zhang, F. He, *Angew. Chem. Int. Ed.* 2021, **60**, 3238-3246.
[S5]H. Lai, H. Chen, Y. Zhu, L. Chen, H.-H. Huang, F. He, *J. Mater. Chem. A* 2020, **8**, 9670-9676.
[S6]Z. Luo, R. Ma, T. Liu, J. Yu, Y. Xiao, R. Sun, G. Xie, J. Yuan, Y. Chen, K. Chen, G. Chai, H. Sun, J. Min, J. Zhang, Y. Zou, C. Yang, X. Lu, F. Gao, H. Yan, *Joule* 2020, **4**, 1236-1247.
[S7]T. Liu, Y. Zhang, Y. Shao, R. Ma, Z. Luo, Y. Xiao, T. Yang, X. Lu, Z. Yuan, H. Yan, Y. Chen, Y. Li, *Adv. Funct. Mater.* 2020, **30**, 2000456.
[S8]S. Li, L. Zhan, Y. Jin, G. Zhou, T. K. Lau, R. Qin, M. Shi, C. Z. Li, H. Zhu, X. Lu, F. Zhang, H. Chen, *Adv. Mater.* 2020, **32**, 2001160.
[S9]D. Hu, Q. Yang, Y. Zheng, H. Tang, S. Chung, R. Singh, J. Lv, J. Fu, Z. Kan, B. Qin, Q. Chen, Z. Liao, H. Chen, Z. Xiao, K. Sun, S. Lu, *Adv. Sci.* 2021, **8**, 2004262.
[S10] S.-S. Wan, X. Xu, Z. Jiang, J. Yuan, A. Mahmood, G.-Z. Yuan, K.-K. Liu, W. Ma, Q. Peng, J.-L. Wang, *J. Mater. Chem. A* 2020, **8**, 4856-4867.